University of Reading

Sensitivity of Philippine historically damaging tropical cyclone events to surface and atmospheric temperature forcings

Article

Published Version

Creative Commons: Attribution 4.0 (CC-BY)

Open Access

Delfino, R. J., Hodges, K. ORCID: https://orcid.org/0000-0003-0894-229X, Vidale, P. L. ORCID: https://orcid.org/0000-0002-1800-8460 and Bagtasa, G. (2024) Sensitivity of Philippine historically damaging tropical cyclone events to surface and atmospheric temperature forcings. Regional Studies in Marine Science, 77. 103595. ISSN 2352-4855 doi: 10.1016/j.rsma.2024.103595 Available at https://centaur.reading.ac.uk/111012/

It is advisable to refer to the publisher's version if you intend to cite from the work. See Guidance on citing.

To link to this article DOI: http://dx.doi.org/10.1016/j.rsma.2024.103595

Publisher: Elsevier

All outputs in CentAUR are protected by Intellectual Property Rights law, including copyright law. Copyright and IPR is retained by the creators or other copyright holders. Terms and conditions for use of this material are defined in

the End User Agreement.

www.reading.ac.uk/centaur

CentAUR

Central Archive at the University of Reading

Reading's research outputs online

Regional Studies in Marine Science 77 (2024) 103595

Contents lists available at ScienceDirect

Regional Studies in Marine Science

journal homepage: www.elsevier.com/locate/rsma

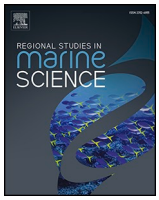

Sensitivity of Philippine historically damaging tropical cyclone events to surface and atmospheric temperature forcings

Rafaela Jane Delfino [a,b,*], Kevin Hodges [b], Pier Luigi Vidale [b], Gerry Bagtasa [a]

[a] Institute of Environmental Science & Meteorology, University of the Philippines-Diliman, Quezon City, Philippines
[b] Department of Meteorology, University of Reading, Reading, United Kingdom

ARTICLE INFO

Keywords:
Tropical cyclones
Sea surface temperature
Global warming
The Philippines
WRF

ABSTRACT

As the climate warms, sea surface temperature (SST) is projected to increase, along with atmospheric variables which may have an impact on tropical cyclone (TC) properties. Climate models have well-known errors in simulating current climate SSTs that will likely affect future TC projections. Therefore, a better understanding of the impact of SST changes will help us identify the largest uncertainty in projecting TC changes. This study employs three different and independent methodologies to investigate the impact of sea surface and atmospheric temperature changes and tropical cyclone (TC) characteristics, focusing on three historically damaging TCs in the Philippines: Typhoons Haiyan, Bopha, and Mangkhut. These methodologies include initially simulations with uniform SST anomalies between −4 to +4°C, then experiments using delta from CMIP6 CESM2 for SST and atmospheric temperature in the far future, and, finally, simulations imposing Radiative-Convective Equilibrium (RCE) conditions. The experiments reveal significant insights into TC dynamics under varying environmental conditions. Changes in SSTs resulted in changes in TC track, intensity, and rainfall. In the positive SST simulations, TCs tended to move northwards and resulted in substantial increases in maximum wind speeds reaching a difference of up to 10, 13, 23 ms^{-1} for Typhoons Haiyan, Bopha, and Mangkhut, respectively. Analysis of the accumulated rainfall also showed that increased SST results in increased rainfall. Inclusion of atmospheric warming offsets the intensification due to SST change. Moreover, warmer SSTs resulted in slower-moving TCs and increased TC size. Further analyses incorporating atmospheric temperature adjustments derived from CESM2 and RCE simulations offer better insights on TC response. Under near-RCE conditions, TCs exhibit reduced sensitivity to SST changes, with smaller intensity and size modifications simulated when stable relative humidity is imposed. The smaller changes in TC intensity and size observed in these experiments suggest that maintaining atmospheric stability through pre-storm atmospheric adjustments dampens the response of TCs to SST warming.

1. Introduction

Tropical cyclones (TCs) are the most destructive extreme weather events in the Philippines. The country receives an annual average of nine landfalling TCs with a total of 19–20 TCs (Cinco et al. 2016) entering the Philippine Area of Responsibility (PAR) which is bounded by the coordinates: 5°N 115°E, 15°N 115°E, 21°N 120°E, 25°N 120°E, 25°N 135°E and 5°N 135°E. These TCs bring intense winds, extreme precipitation, and storm surges that affect a large portion of the Philippines (Bagtasa, 2017; Lyon and Camargo, 2009). On average, the annual financial cost due to TCs amounts to about USD 20 billion in damages, with an estimated affected population of about 5 million people (Brucal et al., 2020) and an average death toll of 885 (Yonson et al., 2016). As a result, the Philippines is one of the countries that are most at risk from climate change where TC-associated impacts are expected to increase with a warming climate (Scoccimarro, 2016, Delfino et al. 2023). Recent research on the effects of climate change on TCs at the global and basin level project an increase in the number of intense TCs (Knutson et al., 2019, Walsh et al., 2019, Christensen et al., 2013, Ying et al., 2012). The same changes are projected to occur in the Philippines region (Gallo et al., 2019). Therefore, an improved understanding of how TCs in the Philippines might change is essential (Villafuerte et al., 2021).

To assess the changes in TC characteristics with a warming climate, several approaches have been used based on global and limited area model simulations of idealized and real TC cases. The first approach is to uniformly change the SSTs while keeping the atmospheric temperature

* Corresponding author at: Institute of Environmental Science & Meteorology, University of the Philippines-Diliman, Quezon City, Philippines.
E-mail address: rpdelfino@up.edu.ph (R.J. Delfino).

https://doi.org/10.1016/j.rsma.2024.103595
Received 18 December 2023; Received in revised form 23 April 2024; Accepted 24 May 2024
Available online 3 June 2024
2352-4855/© 2024 The Authors. Published by Elsevier B.V. This is an open access article under the CC BY license (http://creativecommons.org/licenses/by/4.0/).

constant. For example, SST experiments for TC cases have previously been conducted in other ocean basins such as Typhoon Yasi in Australia (Lavender et al., 2018); Hurricane Catarina in the South Atlantic (Radu et al., 2014); Hurricane Katrina in the US (Kilic and Raible, 2013); Hurricanes Ivan and Katrina (Trenberth et al., 2018) also in the US; and Typhoon Man-yi in Japan (Hegde et al., 2016). These idealized SST experiments were performed to better understand the influence of the SSTs (all other variables held the same) on TCs. However, there is an important caveat in this type of simulation that needs to be considered when interpreting such experiments. Changing the SST without changing the other surface and atmospheric variables will result in imbalances in the surface energy and atmospheric dynamical balance which will affect how TCs are simulated (Nakamura et al., 2017; Lavender et al., 2018). Lavender et al. (2018) found that using warmer SSTs, without modifying the atmospheric temperature, had little influence on the track of Typhoon Yasi but had a significant influence on intensity, rainfall, integrated kinetic energy, and TC-associated storm surge. Radu et al. (2014) conducted simulations of Hurricane Catarina and found a linear relationship between TC size and surface latent heat flux as SSTs and atmospheric temperature are increased. Kilic and Raible (2013) also found a linear relationship between SST and TC intensity based on SST sensitivity experiments of Hurricane Katrina. The alternative approach is to impose both SST and atmospheric temperature changes.

Past and future changes in TC activity are often studied using coupled General Circulation Models (GCMs). However, given the high computational cost required to run high-resolution coupled GCMs to resolve important TC processes (Walsh et al., 2015) as well as their biases in representing SSTs, various strategies have been used to investigate potential changes in TCs in the future. One such strategy is the use of Limited Area Models (LAMs) and the selection of specific TCs from long climate model simulations or that have been observed and then re-simulating them in the higher resolution LAM using relatively small domains and the GCM boundary conditions to capture their intensities better (Bender et al., 2010; Knutson, 1998); or using LAMs with larger domains forced at their boundaries by large scale environmental conditions from GCMs or reanalyses or forced with idealized large-scale environments (e.g., with fixed SSTs) (Hill and Lackman, 2011; Knutson and Tuleya, 2004). More specifically, the Pseudo-Global Warming (PGW) Technique can be used to simulate TCs under different climate conditions by imposing or prescribing SSTs, atmospheric temperature, humidity, and other variables in the initial and lateral boundary conditions derived from one or more GCMs or reanalyses. This approach is used here as well as in a series of works by the same authors (Delfino et al. 2022, 2023) and have been applied by various studies on TCs in different basins i.e., Lackmann, 2015; Takayabu et al. 2015; Ito et al. 2016; Nakamura et al. 2016; Parker et al. 2018; Patricola and Wehner, 2018; Kanada et al. 2021.

Prescribing SST values will likely lead to changes in the stability of the lower atmosphere, which affects the development of convection and, ultimately, the intensification of the TC and its associated rainfall. As a result, the observed changes in TC characteristics may not be realistic (Lavender et al., 2018). To account for these imbalances, the third approach is to start the simulations in the Radiative-Convective Equilibrium (RCE) state (Wang and Toumi, 2018) where storms are simulated under sea surface warming with pre-storm atmospheric adjustments under RCE conditions. Wang and Toumi (2018) showed that the intensity and size of the TC is less sensitive to an adjusted environment under RCE. On a more practical level, running the TCs under RCE conditions will provide for a more realistic increase in mid-level moisture and, therefore, less dramatic increases in TC intensity and size.

As the climate changes and with the Philippines highly exposed to TCs, studies looking at the sensitivity of TCs in the PAR to surface and atmospheric warming are important. With the uncertainties in the accuracy of observed SSTs (Goddard et al., 2009) and SST biases in GCMs (Mejia et al., 2018), it is possible that understanding the sensitivity of TCs to SSTs and atmospheric temperature (ATM) could aid in reducing the uncertainty associated with changes in TC in a warming world (Roberts et al., 2020). Coupled GCMs have well-known errors in simulating current climate SSTs, which are likely to affect future projections. In fact, there is large structural uncertainty in the way that these SSTs are projected, which justifies understanding the impact of an idealised change in SSTs in the present study. This study aims to identify what the largest uncertainties in projecting TC changes are, studying each one in isolation. Moreover, the fact that several recent typhoons that impacted the Philippines occurred in above-average SSTs makes it important to understand how these TCs might have been and will be affected by warmer SSTs. The novelty of the study reported here is in simulating TCs that affected the Philippines, using a LAM at high-resolution coupled to a one-dimensional ocean mixed layer model, and imposing SST warming/cooling as well as atmospheric warming/cooling to understand their contribution to changes in TC properties. The overall objective of this study is to understand the response of Philippine TC cases to sea surface and atmospheric forcings. However, this study does not aim to be a full Pseudo Global Warming (PGW) study (which is the subject of Delfino et al., 2023) but aims to understand the mechanisms involved in possible changes in TCs due to changes in SSTs. This study will also provide additional insights into how the damage potential of TCs may change in a warmer climate. While Comiso et al. (2015) looked at the response of Typhoon Haiyan in the Philippines to above-normal SSTs, no other studies of this type have focused on the response of TCs to prescribed increasing or decreasing SSTs in the Philippines, as considered here. To also add a new dimension to the existing literature, the study reported here focuses on different intensity categories, months of occurrence, and landfall regions in the selection of TC cases.

By using highly idealised simulation setups, this paper attempts to answer the following questions:

- What is the response of TCs to imposed uniform changes in SSTs?
- How do combined surface and atmospheric warming affect the TC characteristics?
- Will the changes in intensity and size be as much as when the TCs are run under RCE conditions?

These questions will be addressed by performing simulations using the Weather Research and Forecasting (WRF) model (Skamarock et al., 2008), a limited area model that has been commonly used in other similar studies, for three of the most damaging TCs that affected the Philippines - Typhoons Haiyan, Bopha, and Mangkhut. The paper continues with a description of the methodology. Section 3 provides the results of the sensitivity experiments, and finally, Section 4 provides a summary of the findings and recommendations for future work.

2. Methods and data

2.1. Case studies: Brief description

The three most damaging (in terms of economic losses) TCs to have affected the Philippines in the 1970–2020 period (Lara, 2020) – were Typhoon Haiyan (2013), Typhoon Bopha (2012) and Typhoon Mangkhut (2018) – see Table 1. Typhoons Haiyan and Bopha are also in the top five deadliest TCs in recorded history. These TC cases were also selected to represent the three main regions of landfall (Fig. 1) – Luzon (Mangkhut), Visayas (Haiyan), and Mindanao (Bopha).

2.1.1. Typhoon Haiyan

Typhoon Haiyan (locally named Yolanda) was classified as a category-5 equivalent super typhoon by the Joint Typhoon Warning Center (JTWC) and was classified as a Typhoon, the highest category in the classification system at the time, by Philippine Atmospheric, Geophysical and Astronomical Services Administration (PAGASA - Philippine National Weather Agency). It intensified and reached its peak

Table 1
Brief Description of the TC Cases - the simulation period, observed minimum central pressure, landfall region, ENSO condition and the cost of damages.

TC case study International (local) name and year	Simulation Period	Minimum pressure	Landfall Region (Latitude of formation)	Domain maximum SST from ERA5 at initialization (global mean obs monthly SST anomaly* & ENSO conditions**)	Cost of Damage***
Haiyan (Yolanda) 2013	04 Nov 00UTC –12 Nov 00UTC	895 hPa	Visayas (5.8 deg N)	30.5 °C (0.58, Neutral)	₱95.5 B/ $2.2B
Bopha (Pablo) 2012	02 Dec 00UTC – 10 Dec 00UTC	930 hPa	Mindanao (3.4 deg N)	28 °C (0.47, mod LN)	₱43.2B/ $1.06B
Mangkhut (Ompong) 2018	10 Sep 00UTC – 17 Sep 00UTC	905 hPa	Northern Luzon (11.8 deg N)	30.6 °C (0.69, weak EN)	₱33.9B/ $627 M

Legend: *global mean observed monthly SST anomaly (Source: NOAA, 2018, 2021); ** ENSO conditions (LN: La Nina; EN: El Nino) (Source: CPC 2021) and *** estimated cost of damage in agriculture and infrastructure (Source: NDRRMC, 2012)

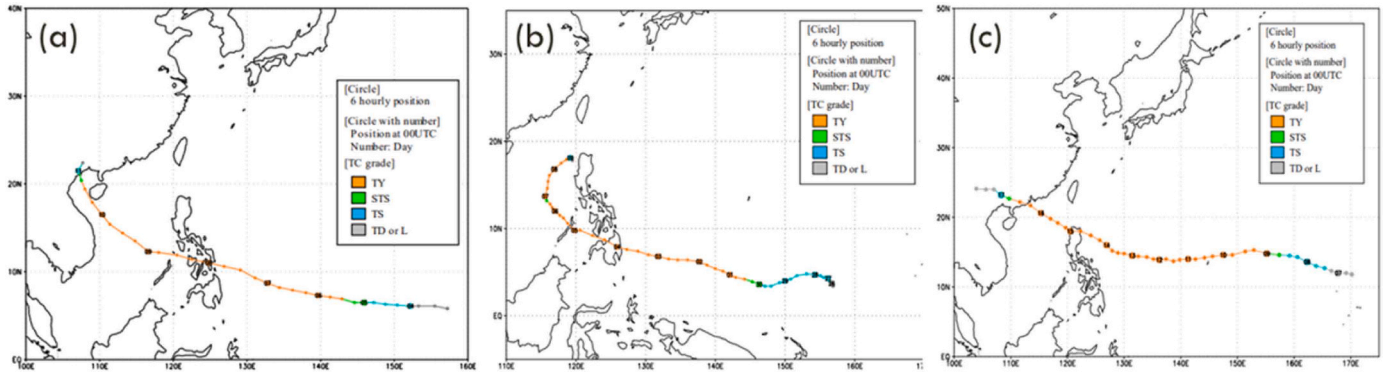

Fig. 1. Observed tracks of the tropical cyclone case studies: (a) Haiyan (November 2013), (b) Bopha (December 2012), and (c) Mangkhut (September 2018), Source: Japan Meteorological Agency (JMA), 2012; Japan Meteorological Agency (JMA), 2013; Japan Meteorological Agency (JMA), 2018

intensity of 87 m/s (1 min-averaged) or 85 m/s (10-min averaged) before making landfall on November 7, 2040 UTC which claimed the lives of more than 6300 people, mostly due to the associated storm surge and coastal inundation. It is estimated to have caused between USD 5–15 billion worth of direct damage to agriculture and infrastructure (Brucal et al., 2020) and affected more than 16 million people (NDRRMC, 2014). Typhoon Haiyan formed in an environment with anomalously high SSTs (peaking at 30.1°C in November 2013, 0.8°C higher than average SST for November in the warm pool region), which was considered the highest observed during the period between 1981 and 2014 in the Warm Pool Region (Comiso et al., 2015).

2.1.2. Typhoon Bopha

Bopha (locally known as Pablo) made landfall over Baganga, Mindanao on December 3, 2012, at 2100 UTC (PAGASA, 2012). It traversed over Mindanao and was downgraded to severe tropical storm intensity over the West Philippine Sea on 6 December at 18 UTC. It re-intensified and was upgraded to typhoon intensity six hours later before turning north-eastward over the sea west of Luzon. Bopha rapidly weakened late on December 8, 2012, and remained almost stationary over the same waters. It gradually weakened and dissipated on December 9, 2012. The heavy rainfall brought by Typhoon Bopha caused a massive debris flow that killed 1248 people in Mindanao and caused an estimated USD 1.06 billion worth of damages to agriculture and infrastructure (NDRRMC, 2012). The global monthly mean SST in December 2012 was 0.47°C higher than the normal December mean SST (NOAA, 2012), hence Bopha formed in a region of higher-than-normal SST.

2.1.3. Typhoon Mangkhut

Typhoon Mangkhut (locally known as Ompong) made landfall in the northern region of the Philippines, over Baggao, Cagayan at 1740 UTC on September 15 as a Typhoon (PAGASA, 2018). Interaction with the rugged terrain of Northern Luzon after landfall caused the typhoon to weaken significantly after traversing Luzon. The global monthly mean SST in September 2018 was 0.69°C higher than the normal September mean SST (NOAA, 2018), associated with a weak El Nino event (CPC, 2019). Hence Mangkhut formed in a region of higher-than-normal SST (NOAA, 2018). The typhoon caused widespread damage across Northern, Central, and parts of Southern Luzon due to its intense nature and large size (~ 900 km). It affected more than 700,000 families (or close to 3 million people) with 138 injured and 68 dead. The estimated direct damage to infrastructure and agriculture was around USD 623 million (NDRRMC, 2018).

2.2. Data

The European Centre for Medium-Range Weather Forecasts (ECMWF) Re-analysis 5th Generation (ERA5) is used for both the initial and 6-hourly boundary conditions of the WRF simulations. It is the latest generation of reanalysis products produced by ECMWF with a horizontal resolution of 31 km, hourly temporal resolution, and 137 atmospheric levels (Hersbach et al., 2020). ERA5 utilizes the best available observational data from satellites and in-situ stations, which are quality controlled and assimilated using a state-of-the-art 4-dimensional data assimilation system (4D-VAR) (Isaksen et al., 2010) and the ECMWF's Integrated Forecast System (IFS) Cycle 41r2. The observed TC data used here is the best-track information taken from the World Meteorological Organization (WMO) subset of the IBTrACS (IBTrACS-WMO, v03r09) (Knapp *et al.,* 2010) which is the best-track data provided by the Japan Meteorological Agency (JMA).

2.3. Model configuration

Numerical simulations were conducted using the WRF version 3.8.1 (Skamarock et al., 2008). This is a regional non-hydrostatic atmospheric model developed by the National Center for Atmospheric Research (NCAR), used for atmospheric research and operational forecasting, and increasingly for regional climate research (Powers et al., 2017). The

physical parameterization schemes available in WRF to represent un-resolved processes include cumulus convection, microphysics, radiative transfer, planetary boundary layer (PBL), and land surface each of which has a selection of different methods. The Advanced Research WRF (ARW) solver uses the Arakawa-C grid as the computational grid and the Runge-Kutta 3rd-order time integration schemes (MMML-NCAR, 2019). The model features are described in more detail in Skamarock et al. (2008).

In this study, the WRF–ARW model has been configured with two nested domains centered over the point of 18.3° latitude and 135° longitude. The outermost grid has 294 ×159 grid points with 25 km grid spacing, while the innermost domain has 745 ×550 grid points with 5 km grid spacing, with 44 vertical eta levels and the model top pressure level was set to 50 hPa. The results shown here are from the inner 5-km domain. This model resolution was chosen based on previous sensitivity experiments which found that this resolution can capture the track and intensity of the TC cases well (Delfino et al., 2022). See Delfino et al., (2022) for more details on the model configuration.

The parameterization schemes used in the model are the same as Delfino et al. (2022) which examined the sensitivity of the representation of the TCs to different parameterisations which led to the choices used here, in particular, the Kain-Fritsch scheme for the cumulus parameterization, which was found to simulate the TC track and intensity well. Other parameterizations were adopted from Li et al. (2018) i.e. the Rapid Radiative Transfer Model (RRTM) scheme (Mlawer, et al., 1997) and the Dudhia scheme (Dudhia, 1989) for the longwave and shortwave radiation, respectively; the surface layer uses the MM5 Monin- Obukov scheme (Monin and Obukhov, 1954); the WRF Single–moment 6–class Scheme for the cloud microphysics (Hong and Lim, 2006); and the Yonsei University (YSU) PBL scheme (Hong *et al.*, 2006); and the land surface processes and structure are defined by the Unified Noah Land Surface Model (Chen and Dudhia, 2001; Tewari et al., 2004). The same parametrizations were used in both the outer and inner domains.

The simple mixed-ocean layer (one-dimensional, 1D) model capability in WRF is used to capture the TC-induced SST cooling, wherein an initial mixed-layer depth was set to 50 m and the temperature lapse rate below the mixed layer to 0.14 °C m^{-1}. The surface flux option 1 in WRF was used (as described in Kueh *et al.* 2021) which was found to simulate TC intensities better (Delfino et al., 2022). We have opted to use the 1D ocean model since recent studies suggest that this may be sufficient to capture most of the TC-induced SST cooling while retaining the anomalous forcing (as also illustrated in Supplementary Figure 1 based on our simulations for the three TC cases) in the region providing heat energy to the TC (Yablonsky and Ginis, 2009). In addition, compared to coupled models that contain a fully three-dimensional (3D) ocean component, WRF's 1D model can save valuable computational resources. The 1D model, however, does not capture upwelling which may lead to the underestimation of sea surface cooling along the TC core (Yablonsky and Ginis, 2009).

2.4. TC tracking method

The simulated track and intensity values were obtained every 6 hours using the TRACK algorithm (Hodges et al., 2017) as used in Hodges and Klingaman (2019). TRACK determines TCs as follows: first, the relative vorticity at 850-, 700-, and 600-hPa levels are obtained and averaged. The field is then spatially filtered using 2D discrete cosine transforms equivalent to T63 spectral resolution and the large-scale background is removed. The feature points are determined by first finding the grid point relative vorticity maxima $> 5.0 \times 10^{-6}$ s^{-1} which are then used as starting points for a B-spline interpolation and steepest ascent maximization method, to determine the off-grid feature points (Hodges 1995 as cited by Hodges and Klingaman, 2019), this results in smoother tracks. The feature points are initialized into tracks using a nearest neighbour method and then refined by minimizing a cost function for track smoothness subject to adaptive constraints on track smoothness and displacement distance in a timestep (Villafuerte et al., 2021). The tracking is done for the entire simulation period. After completing the tracking, other variables are added to the tracks, including the maximum 10-m winds and minimum central pressure at full resolution. This is done by searching for the maximum 10-m winds within a 6^0 geodesic radius, and for the true pressure minimum within a 5^0-radius using the B-splines and minimization method (Hodges and Klingaman, 2019).

2.5. Changes in environmental fields

Metrics were calculated for the different environmental fields that may influence the TC characteristics including the latent heat flux, water vapor mixing ratio, simulated mid-tropospheric (700–500hPa) relative humidity, and vertical wind shear averaged over the entire period of the simulation and in the entire inner domain.

The simulated deep layer vertical wind shear was calculated as:

$$\textit{Vertical Wind Shear} = \sqrt{(u200 - u850)^2 + (v200 - v850)^2}, \quad (1)$$

where *u, v* are the zonal and meridional wind components, respectively, at 200 and 850 hPa. The time-averaged vertical wind shear has been calculated from u and v winds at 200 and 850 hPa at each grid point.

2.6. Experimental set-up

2.6.1. SST experiments

There are a total of eight SST experiments per TC case (Table 1), all of which used the ERA5 data for initial and boundary conditions. The initialization times were chosen based on preliminary sensitivity experiments (Delfino et al. 2022). First is the control run (CTRL) that uses the ERA5 SSTs followed by the set of six experiments with an imposed SST anomaly of −4, −2, −1, +1, +2, +4 °C (denoted as SST-4, SST-2, SST-1, SST+1, SST+2 and SST+4) across the whole outer domain per TC case. The experiments performed for this study use a similar methodology to that of Lavender et al. (2018) and Radu et al. (2014). Typhoon Haiyan was simulated from 04 Nov 00UTC to 12 Nov 00UTC, Bopha from 02 Dec 00UTC – 10 Dec 00UTC, and Mangkhut from 10 Sep 00UTC – 17 Sep 00UTC for each of the experiments.

2.6.2. GCM-based SST and ATM delta experiments

To compare with the idealized experiments, an additional set of simulations were performed using the monthly mean SST delta, or the difference between the historical and current environment/climate imposed on the ERA5 initial and boundary conditions, from one representative CMIP6 coupled GCM – The Community Earth System Model Version 2 (CESM2) (Danabasoglu et al., 2020) (denoted as +CESM2) for the far-future period of 2070–2099 and the worst-case/high-emission scenario, Shared Socio-economic Pathways (SSP)5–8.5. CESM2 was evaluated to have relatively good performance in simulating the spatial pattern of the climatological mean SST in the WNP Basin (Han *et al.*, 2021). Fig. 2 shows the imposed monthly mean SST deltas. Based on the future climate change signals calculated from the CESM2, the mean SST change is projected to be between 1.89°C to 3.65°C warmer with a mean monthly delta of 3.22°C, 1.09°C, and 2.94°C for November, December, September in the far future under the SSP5–8.5 scenario, respectively. The simulations were run for the same length of simulation to cover the TCs lifetime per TC case (Table 1) using the same set of parameterizations. The only difference among the simulations is the SSTs added or subtracted at the initial and bottom boundary condition. The other variables in the initial and lateral boundary conditions, including relative humidity, were kept the same in all experiments.

Three additional model simulations were performed to test the sensitivity of the TCs to perturbations of both the SST and atmospheric temperature profile. In each experiment, the SST and the atmospheric

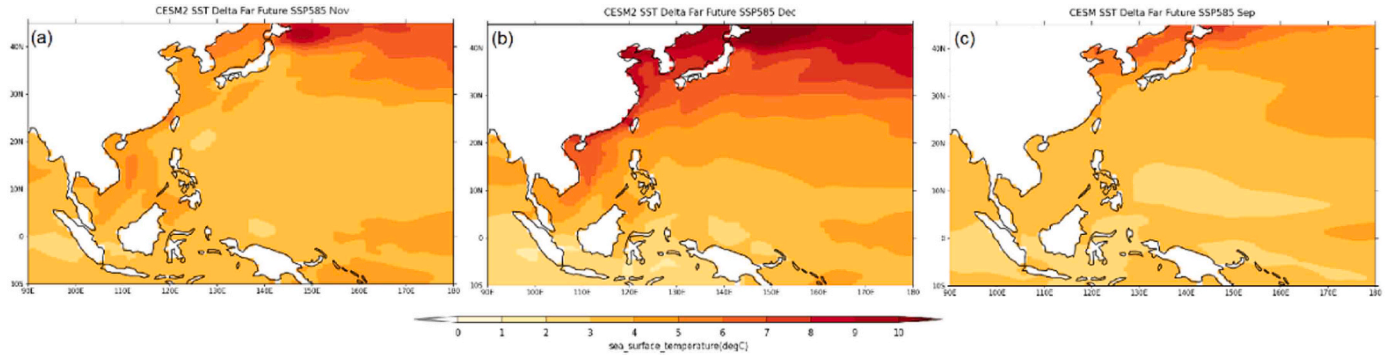

Fig. 2. The (a) November, (b) December, and (c) September monthly mean sea surface temperature delta (°C) added to the boundary and initial conditions of the CTRL runs for Typhoons Haiyan, Bopha, and Mangkhut, respectively, to create the future climate scenario change in far future (2070–2099) from CMIP6 CESM2 model according to the SSP5–8.5 scenario relative to the historical period (1970–1999) [denoted as +CESM2 experiments].

temperature profiles, were perturbed based on the mean atmospheric profile changes from the CESM model for the far-future period of 2070–2099. The other variables in the initial and boundary conditions, including relative humidity, were kept the same in all experiments. It is important to note that since we increased the atmospheric temperature profile at the boundaries, the atmospheric moisture is expected to increase (Schär et al., 1996; Lenderink et al., 2019), as a consequence of increasing the water vapour saturation (Radu et al., 2014).

2.6.3. Radiative-convective equilibrium (RCE) experiments

Additional experiments were also performed to study the impact of the imbalances created by only adjusting the SST. Based on previous studies (Wang and Toumi, 2018; Nolan et al., 2007), there is a considerable variation in how TC intensity responds to changes in SST when considering whether or not a pre-storm RCE adjustment is in place. Furthermore, it remains unclear how the size of TCs responds to SST changes under RCE conditions over a timespan similar to actual TCs. To cover these sensitivities, we tried to investigate them in this study by simulating the TCs under RCE conditions. Experiments with SST warming of 2C with additional spin-up time of 15 days (for Haiyan only, SST+2_-15days), 10 days (SST+2_-10days) and experiments under stable relative humidity (SST+2_rh) for the three TC cases were performed (Table 2). To keep the relative humidity stable in the domain, spectral nudging was applied for the horizontal and vertical wind components, the potential temperature, and the geopotential height using ERA5. The nudging coefficients for all variables were set at 0.0003 s^{-1}, applied at all levels above the PBL.

The criterion for RCE is that the potential temperature at each vertical layer below 200 hPa does not change more than 1 K in the next 30 simulation days, which is a similar criterion as used in Chavas and Emanuel (2014). The duration to reach the RCE state may vary with different RCE definition criteria (Tompkins and Craig, 1998). As shown in Fig. 3 below, the RCE criterion is partly achieved in the SST+2 experiments after approximately 12 days of simulation in the −15 days experiments for Typhoon Haiyan.

3. Results and discussion

3.1. Influence of uniform delta SST on TC characteristics

3.1.1. Simulated track and size

Fig. 4 shows the track obtained from the observations (IBTraCS), the CTRL simulation, and the perturbed SST simulations (-4, −2, −1, +1, +2, +4). The change in SSTs results in differences in the simulated tracks, and landfall areas. The positive change SST simulations have a general tendency for the TCs to move northwards relative to the CTRL run, and for some, to recurve north and not make landfall over the Philippines, while the negative change SST simulations have a tendency for the TCs to move southwards relative to the CTRL run. The simulations with SST+4 for Typhoon Haiyan (Fig. 4a) and SST+1, SST+2, and SST+4 experiments for Typhoon Mangkhut (Fig. 4c) recurve and do not

Table 2
List of the experiments.

Simulation Group / Code	TC Cases	Simulation Period	Variables	Uniform delta / change
Set A. Uniform SST delta experiments				
Control (CTRL)	Haiyan	Haiyan 04Nov 00UTC – 12Nov 00UTC	n/a	
SST-	Bopha	Bopha 02Dec 00UTC −10 Dec 00UTC	SST	-4
	Mangkhut	Mangkhut 10Sep 00UTC – 17Sep00UTC		-2
				-1
SST+			SST	+1
				+2
				+4
Set B. GCM-based SST + ATM delta experiments				
+CESM2_SST	Haiyan	Haiyan 04Nov 00UTC – 12Nov 00UTC	SST	
+CESM2_SST+ATM	Bopha	Bopha 02Dec 00UTC −10 Dec 00UTC	SST+ATM	
	Mangkhut	Mangkhut 10Sep 00UTC – 17Sep00UTC		
Set C. RCE experiments				
SST+2_-15days	Haiyan	Haiyan 20Oct 00UTC – 12Nov 00UTC	SST	+2
SST+2_-10days	Haiyan	Haiyan 25Oct 00UTC – 12Nov 00UTC	SST	+2
	Bopha	Bopha 22Nov 00UTC −10 Dec 00UTC		
	Mangkhut	Mangkhut 29Aug 00UTC – 17Sep00UTC		
SST+2_rh	Haiyan	Haiyan 04Nov 00UTC – 12Nov 00UTC	SST Spectral nudging first 48 hours for u,v,t,ph; nudging coefficient =0.0003	+2
	Bopha	Bopha 02Dec 00UTC −10 Dec 00UTC		
	Mangkhut	Mangkhut 10Sep 00UTC – 17Sep00UTC		

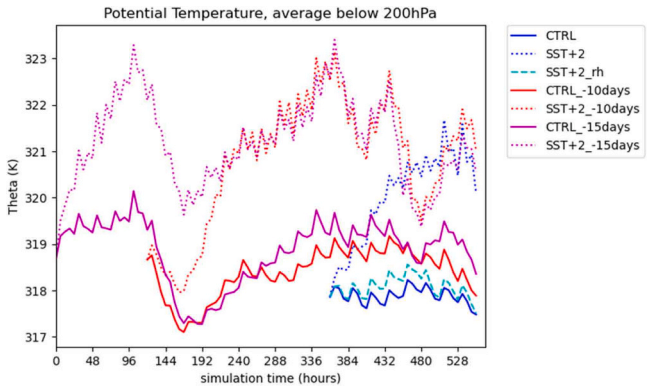

Fig. 3. Average potential temperature (Theta, K) averaged below 200hPa level for the RCE experiments on Typhoon Haiyan (2013). RCE experiments are labelled as follows: with the control (CTRL) with additional spin-up time of 10 and 15 days, SST warming of 2C with additional spin-up time of 15 days (for Haiyan only, SST+2_-15days), 10 days (SST+2_-10days) and experiments under stable relative humidity (SST+2_rh).

make landfall in the Philippines. On the other hand, the SST+1 and SST+2 experiments for Typhoon Haiyan made landfall farther north of the country. The simulated tracks for Typhoon Bopha (Fig. 4b), on the other hand, are similar to the observed landfall areas for the warm SST experiments.

Based on an analysis of the simulated TC track, particularly the northward movement of the TCs when SST are increased, the changes in the TCs are consistent with changes in the large-scale environment (Fig. 5). The most notable of these is the shift in the location of the (western) edge of the Western North Pacific Sub-Tropical High (WNPSH), here represented as the 5800 m gpm contour of the geopotential height at 500hPa. The WNPSH weakens and retreats eastward as SSTs are increased (more retraction in SST+4) which is seen in all three TC cases (Fig. 5). Note, however, that the location of the WNPSH is different among the cases due to the difference in months of occurrence. It is also important to note that the locations of the WNPSH in the CTRL runs are similar to the mean of observations in the months when the TCs occurred. In general, there are changes of a few degrees in the extent of the WNPSH as the SSTs are increased.

The results in this present study provide further evidence to support the conclusions from previous studies on the impacts of SST warming on TC size, and the retraction of WNPSH and TC tracks over the WNP e.g. that of Katsube and Inatsu (2016) where they found that some of the TC cases that occurred in WNP basin between 2002 and 2007 have the tendency to move northward and recurve when 2 K is added uniformly in SST across the domain of a regional atmospheric model. An earlier study by Ren et al. (2014), which looked at the sensitivity of TC tracks and intensity to ocean surface temperature of four different TC cases in four ocean basins including Typhoon Ketsana (2003) in the WNP basin, found that due to warmer SSTs, the WNPSH is further weakened, thus causing Ketsana to move and recurve northward. More recently, Sun et al. (2017a) conducted a numerical investigation on the impact of ocean warming on TC track over the western North Pacific and they showed that simulated TC tracks move northward following SST increases. The mechanisms driving these changes were also elucidated by Sun et al. (2017a), providing additional context to our findings. In more general terms, future climate scenarios suggest a poleward shift in the maximum intensity of TCs over the western North Pacific. According to Cao et al. (2024), this poleward shift may be due to the weakening of the Hadley circulation leading to suppression of TC genesis in the lower latitudes (5–20 North), driven by upper-tropospheric warming and its

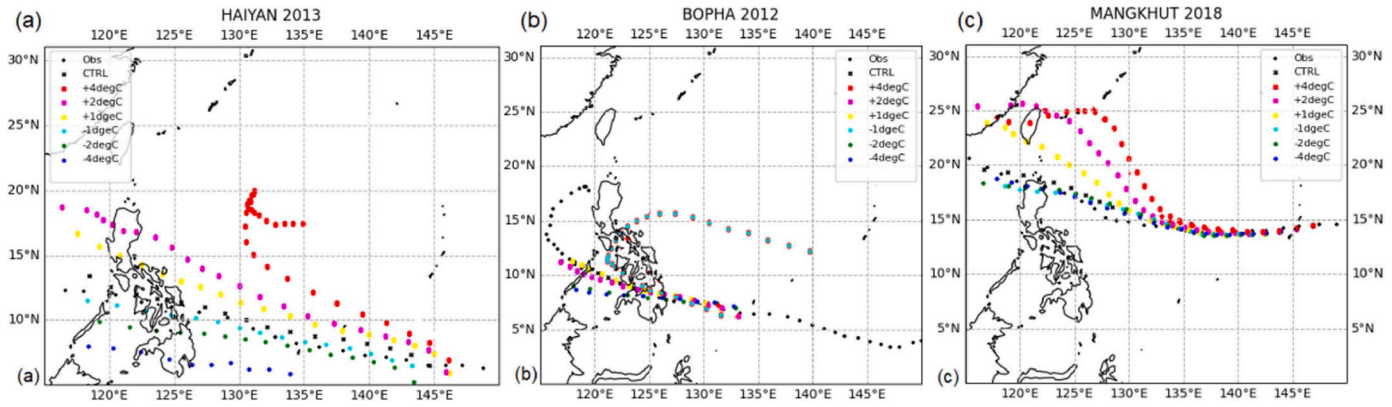

Fig. 4. Simulated tracks from the SST experiments and observed from IBTrACS (obs, black dots) tracks for the different TC case studies - (a) Haiyan (left), (b) Bopha (center) and (c) Mangkhut (right).

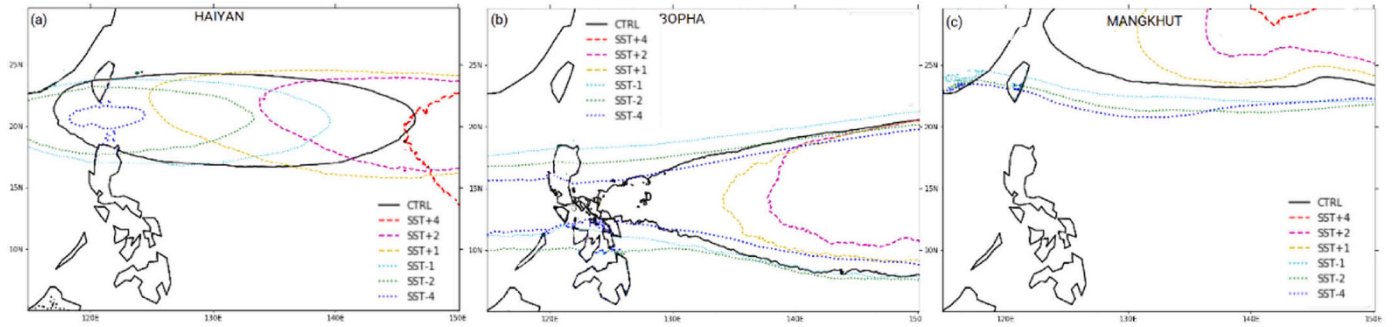

Fig. 5. The coloured dashed(dotted) contours represent the location of the Western North Pacific Sub-tropical High (5800 gpm Geopotential Height at 500hPa) for the positive (negative) SST anomalies; the black solid line contour shows its location for the CTRL simulation.

impact on atmospheric ascent and descent. The descending branch of the Hadley circulation leads to subsidence in the subtropics which can weaken the WNPSH which may then lead to northward re-curvature of TCs.Fig. 6

We defined the TC size in terms of the radius of maximum winds (RMW) and the extent of different wind thresholds as used in Radu et al. (2014) i.e., gale-force winds (GFW, 17.5 m s−1), damaging-force winds (DFW, 25.7 m s−1), and hurricane-force winds (HFW, 33 m/s). The increased SST experiments show an increase in size to up to 60 % in the SST+2 experiments, conversely in the decreased SST experiments, a maximum decrease of 92 % is seen for HFW for the SST-4 run, for Typhoon Haiyan, relative to the CTRL run. The same pattern of changes, an increase (decrease) in TC size with increased (decreased) SST, can be seen for the other two cases (as can also be seen in Supplementary Figures 2–4). Fig. 8 also shows the summary of the changes in size as defined by the different wind thresholds in the different experiments. The area enclosed by the HFW, DFW, and GFW are larger, compared to the CTRL, in the SST+1, SST+2, and SST+4 experiments, and are relatively more pronounced for the TC cases with more extreme winds i.e., Typhoon Haiyan and Typhoon Mangkhut. For Typhoon Haiyan, Bopha and Mangkhut, the radius of HFW is 1.5° (2°), 0.25° (0.25°), and 0.5° (1°) larger in the SST+2 (SST+4) experiments, respectively.

The changes in size are consistent with past SST sensitivity experiments i.e., that of Radu et al. (2014) where the size of Hurricane Catarina increased as SSTs and atmospheric temperature were increased. Sun et al. (2017b) investigated the impact of ocean warming on TC size and destructiveness, revealing that TC size increases with SST, which corroborates our results. In another study, however, Bi and Li (2023) investigated the sensitivity of TC size to SST changes beyond a radius of 200 km from the TC center. They found that increased SST in the outer region negatively affected TC size by enhancing latent heat flux from the sea surface, promoting small-scale convection, and warming the lower and mid-troposphere. This warming altered the local pressure gradient force, weakening the TC's secondary circulation and suppressing spiral rainbands outside the eyewall. Bi and Li (2023) emphasized that outward-propagating rainbands play a critical role in TC size dynamics. The diabatic heating from these rainbands induced inflow at lower levels, facilitating TC expansion.

3.1.2. Simulated intensity

The simulated intensity and the differences in terms of the minimum central pressure and maximum instantaneous 10-m winds between the CTRL and SST experiments and observations are shown in Figs. 6 and 7, respectively. There is a clear and systematic change in the intensities, with larger differences occurring with larger SST differences, particularly for the positive anomalies. Increasing the SST has a large influence on the minimum pressure resulting in storms deeper than observed (Fig. 6, a-c), with a maximum difference relative to the CTRL of up to about 124 hPa in the SST+4 experiments (Fig. 6, d-f) in the entire simulation period, particularly for the stronger TCs –Haiyan and Mangkhut. Typhoon Haiyan's minimum central pressure (Fig. 6a) is 909 hPa in the CTRL run (compared to the observed central pressure of 895 hPa) while the SST+1, SST+2, and SST+4 experiments have minimum pressures of 907hPa, 886hPa, and 846hPa, respectively. For Typhoon Bopha (Fig. 6b), the minimum central pressure reaches 943hPa, 944 hPa, 940 hPa, and 939 hPa in the CTRL, SST+1, SST+2, and SST+4 experiments before landfall, respectively, compared to the observed minimum central pressure of 930 hPa. The minimum central pressure of Typhoon Mangkhut reached 916 hPa, 900hPa, 880 hPa, and 830hPa in the CTRL, SST+1, SST+2, and SST+4 experiments (Fig. 6c) for the entire simulation period, respectively, compared to an observed value of 905hPa. Relatively higher minimum central pressures are simulated with the negative SST anomalies for all three TC cases as compared to the CTRL run.

At peak intensity, the maximum instantaneous surface wind in the CTRL simulation of Typhoons Haiyan, Bopha, and Mangkut reached 68 m/s, 60 m/s, and 63 m/s, respectively (Fig. 7). The observed maximum winds from the best track data reached 64 m/s, 51 m/s, and 57 m/s for Typhoons Haiyan, Bopha, and Mangkut, respectively. Higher maximum wind speeds are simulated in the experiments with positive SST anomalies. The higher maximum wind speeds reach up to 78, 74, and 86 m/s for Haiyan, Bopha, and Mangkhut, for the SST+4 runs,

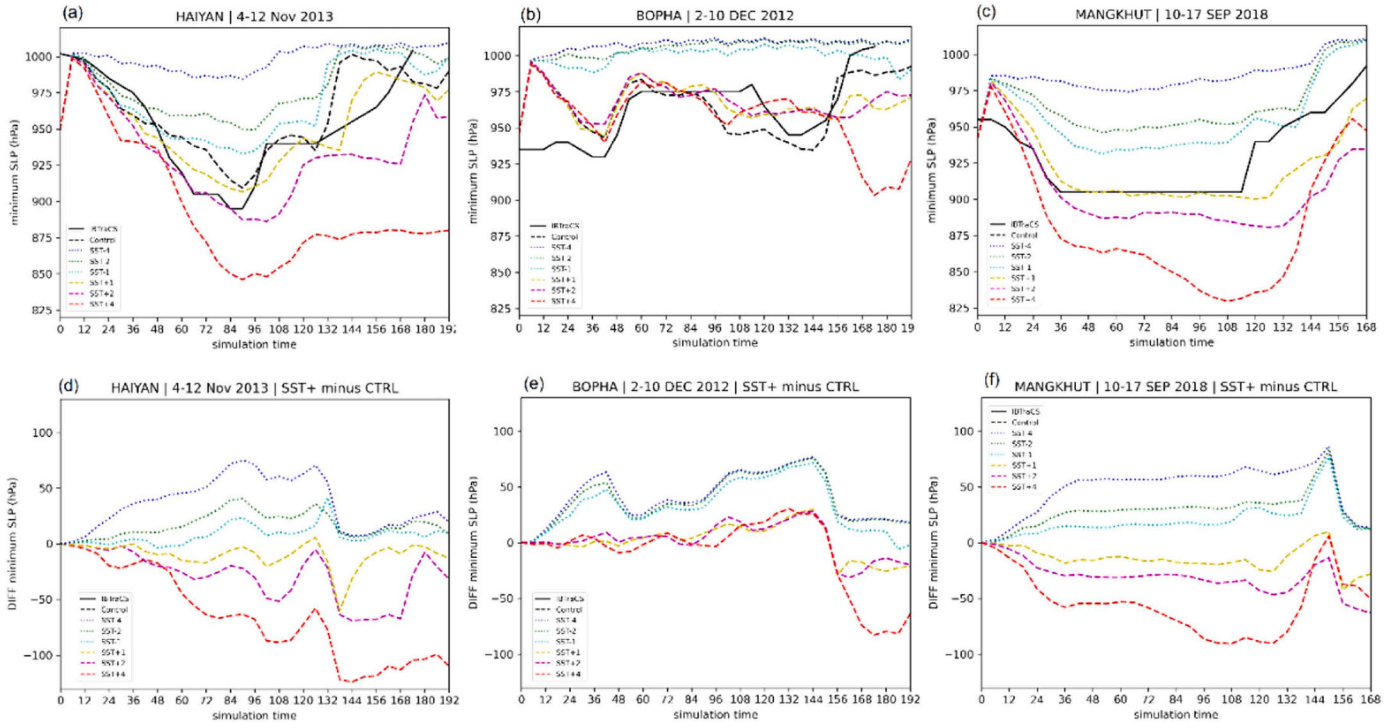

Fig. 6. Time series of the (a-c) minimum central pressure (hPa) and (d-f) the difference between the SST experiments minus CTRL run for Typhoons Haiyan (left), Bopha (center), and Mangkhut (right). The X-axis shows the simulation time from start to end for each TC case.

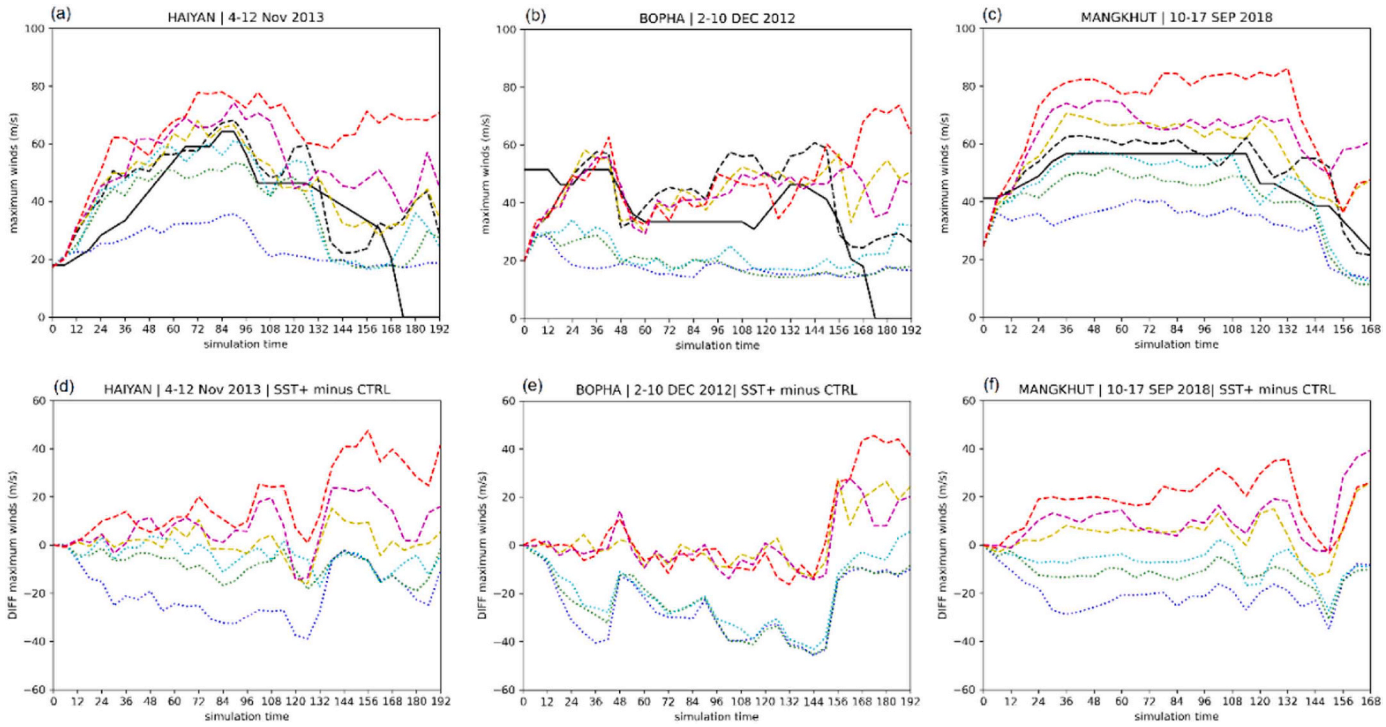

Fig. 7. Same as Fig. 6 but for maximum winds (m/s).

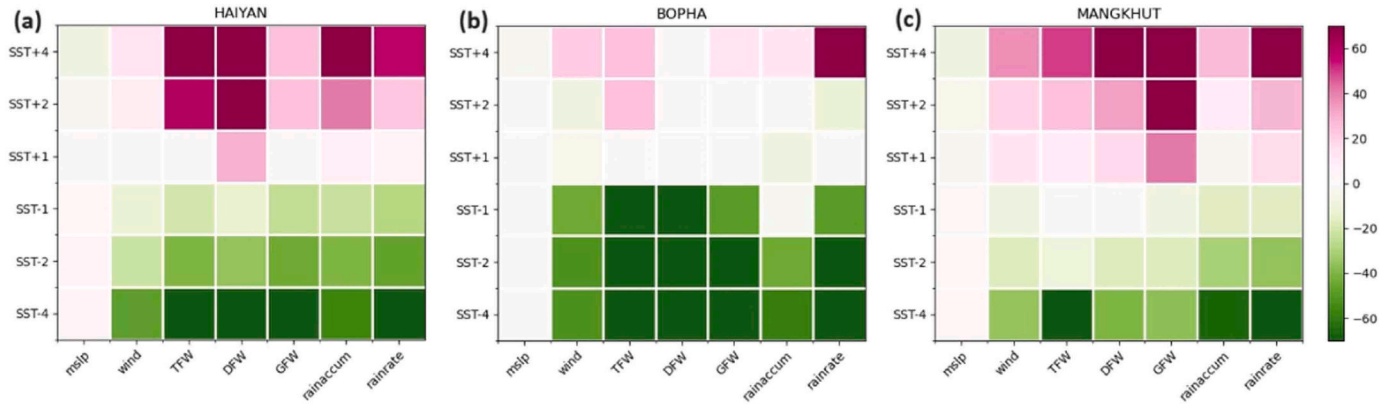

Fig. 8. Percent change relative to the control in TC characteristics in terms of intensity - minimum sea level pressure (mslp); maximum winds (wind); size - typhoon force winds (TFW), damaging force winds (DFW), and gale force winds (GFW); rainfall – total accumulated rainfall (rainaccum) and hourly rainfall rate (rainrate) for the SST+ and SST- experiments for Typhoons (a) Haiyan, (b) Bopha, and (c) Mangkhut.

respectively. The opposite is true with the negative SST anomalies.

The changes in the simulated intensity are consistent with the results of previous SST sensitivity studies i.e., Lavender et al. (2018), Radu et al. (2014) and Kilic and Raible, (2013). Studies by Sun et al. (2013, 2014) also explored the effects of uniform ocean warming on TC intensity. Their findings indicated that TC intensity increases under such conditions, which aligns with our findings. Additionally, Sun et al. (2013, 2014) highlighted the contrasting effects of inner and outer SST on TC intensity which provides further insights into the complexities of this relationship. It is important to note here, however, that Bopha's intensity doesn't reach the observed intensity in the CTRL experiments and the changes in intensity in the SST+ experiments are not as much as that of Haiyan and Mangkhut. The potential mechanisms behind these changes in intensity are discussed in Section 3.1.5.

3.1.3. Simulated rainfall and translation speed

In general, it is expected that in a warmer climate, the precipitation will increase because of the increase in the atmospheric water vapour content (Emanuel *et al.* 2008). In particular, Schär et al. (1996) discussed that if there is a uniform 2 K increase in temperature and the boundary conditions for relative humidity are left unchanged, this will result in a domain-averaged 15 % increase in the atmospheric moisture content. The percent change in maximum and mean accumulated rainfall (entire simulation period) and in the maximum and mean rainfall rate (at landfall) are shown in Fig. 8. The precipitation is averaged over a square box of 5° x 5° around the TC center, which is representative of the area of TC-associated precipitation. The SST+4 experiments achieve the highest percent change in both the accumulated rainfall at peak intensity (reaching up to 87 %, 11 %, and 26 % for Haiyan, Bopha, and Mangkhut, respectively), and rainfall rate (reaching up to 46 %, 86 %, and 35 % for Haiyan, Bopha, and Mangkhut, respectively) among all the SST experiments considered in the study. Several past studies e.g., Hill and Lackmann (2011) and Lavender et al. (2018) have also observed significant increases in the TC-associated rainfall with increased SSTs.

In this study, we found that the most robust increase with additional SST warming is in the TC-associated rainfall with an average increase per degree C of 12 % for Haiyan, 5 % for Bopha and 14 % for Mangkhut in the SST+4 experiments. This result is consistent with previous studies that the TC-associated rainfall rate is projected to increase with global warming, and this is expected to exacerbate TC-associated flood and landslide risk (Knutson et al., 2021; Kossin, 2018; Liu et al., 2019). The IPCC AR6 concluded that it is very likely that "average TC rain rates will increase with warming, and likely that the peak rain rates will increase at greater than the Clausius-Clapeyron scaling rate of 7 % per 1 C of warming in some regions". In a multi-model assessment of TCs, under a +2℃ warming scenario, TC-associated rainfall rates are projected to increase globally by an average of +14 % (+6 to +22 %), with the TC-associated rainfall rate in many individual basins projected to incur similar increases (Knutson et al., 2020). There is general consistency among models in the sign of this projection, globally and at the basin scale (Knutson et al., 2021). In the western North Pacific, studies have projected a +5 to +7 % increase in rainfall rates of typhoons occurring in a warmer climate (Wang et al., 2014; 2015). A more recent assessment report released by the UN ESCAP/WMP Typhoon Committee (Cha et al. 2020) showed that all projections on TC-associated rainfall rates are positive, indicating a tendency for an increase, with a median change of about + 17 %, and a 10th – 90th percentile range of +6 % to +24 % activity in the western North Pacific in a +2℃ warming scenario.

We also looked at the changes in the translation speed of the TC cases since the observed and future changes in speed remains uncertain (Zhang et al. 2020). Slower TCs could mean more time inland and, therefore lead to more exposure; they could also rain for a longer period inland (Bagtasa, 2022). Slower TCs over the ocean would mean that the TC stays longer over warm ocean waters, enhancing the potential for further intensification. Faster moving TCs on the other hand could result in less time for people to prepare. We see slower-moving TCs as SSTs are increased. Haiyan, Bopha, and Mangkhut are 5 %, 8 %, and 2 % slower in the SST+2 simulations compared to the CTRL run, respectively. And slower (24 % for Haiyan, 47 % for Bopha, and 5 % for Mangkhut) for the SST+4 experiments, relative to the CTRL. In a more recent study by Gong et al. (2022), there seemed to be a decreasing trend in TC translation speed from 1980 to 1997 and an increasing trend from 1998 to 2018 over the WNP, in relation to the TC lifetime maximum intensity. The slowing of TC motion near landfall could translate to an increase the damage potential due to greater flood risks (Lai et al., 2020).

In our study, positive SST anomalies resulted in northward TC tracks, intensified TCs, and increased TC size, consistent with previous research by Sun et al. (2017a, 2013, 2014, 2017b). These findings underscore the robustness of the relationship between SST changes and TC behavior, highlighting the importance of considering ocean warming in future TC

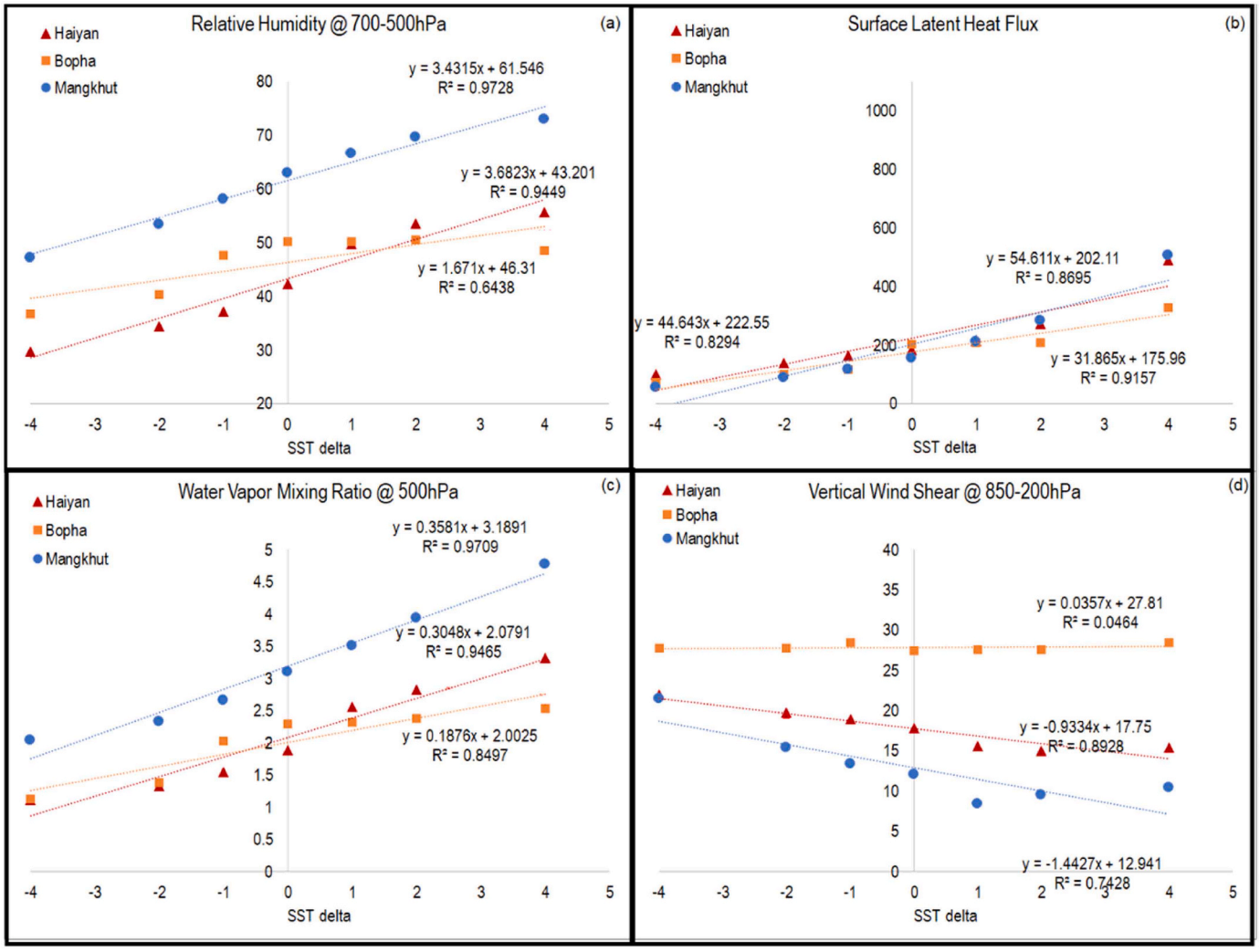

Fig. 9. Changes in TC environment (domain- and time-averaged) in terms of (a) Mid-tropospheric Relative Humidity in %; (b) Surface Latent Heat Flux (W/m2); (c) Water Vapor Mixing Ratio @500 hPa (g/kg); and (d) Vertical Wind Shear @850–200hPa of Typhoon Haiyan (red triangle), Typhoon Bopha (orange box) and Typhoon Mangkhut (blue circle) for the uniform delta SST experiments.

projections.

3.1.4. Changes in environmental variables

In the previous section, we found that the primary changes in the TC cases with changes in SSTs are a northward shift in tracks and a systematic increase in intensity and rainfall when SST is increased. Previous studies have highlighted the effect of warm SSTs on the development and intensification of TCs (Lavender et al. 2018); in particular, surface fluxes of latent and sensible heat from the oceans provide the potential energy for TCs (Emanuel, 1986), thus the increased SST experiments lead to more intense TCs by providing much more surface heat flux, while increases in atmospheric temperature offsets this intensification effect by stabilizing the atmosphere. Fig. 9a shows that relative humidity increases as SST is increased and decreases as SST is decreased. In addition, Figs. 9b and 9c show the average surface latent heat flux (W m-2) and water vapor mixing ratio (g/kg), respectively. The surface latent heat flux and water vapor mixing ratio also increase (decreases) as SSTs are increased (decreased) throughout the simulation period for all TC cases, relative to the CTRL. The average latent heat fluxes are higher in the SST+1, SST+2, and SST+4 experiments compared to the CTRL run, while the flux is reduced in the decreased SST experiments. Besides the increase in SSTs, the increase in wind speeds associated with the increase in SSTs also results in higher latent heat fluxes (Radu et al. 2014). The water vapor mixing ratios are also higher in the SST+1, SST+2, SST+4 experiments compared to the CTRL run starting after 12 hours of simulation up to the end of the simulation period in all three TC cases. This is consistent with the results of Radu et al. (2014). The presence of dry air in the vicinity of the TC is one factor that will hinder intensification. At the same given temperature, dry air is less buoyant than moist air, which limits ascending motion. Furthermore, dry air may also prevent ascending air parcels from reaching saturation, which reduces both the amount of condensation and the amount of latent heat released. In addition, Xu et al. (2016) also found that TC intensification rates are higher when a TC is located in a region with higher SST and lower vertical wind shear (VWS). The VWS in the warmer SST experiments are relatively less than the CTRL experiments for Haiyan and Mangkhut, but the changes in VWS are minimal for Typhoon Bopha (Fig. 9d).

We have also highlighted in the previous section that there are changes in rainfall which can also be explained by the changes in relative humidity and water vapor mixing ratio. In the increased SST experiments, there is a general tendency toward an overall increase in water vapor mixing ratio and in relative humidity (i.e., simulated mid-tropospheric (700–500hPa) relative humidity averaged over the entire period of the simulation) in the entire domain, while there is a reduction in the decreased SST experiments.

3.2. GCM-based SST + ATM delta experiments

To further investigate the response of the TC cases to warming, we have used the second approach wherein changes in the atmospheric temperature profile, calculated from CESM2, were imposed to maintain stability in the lower atmosphere.

Fig. 10 shows that there are pronounced changes in most TC characteristics in the CESM2_SST experiments while there are relatively smaller changes in the CESM2_SST+ATM experiments. This is particularly true in the changes in intensity in terms of minimum sea level pressure and maximum winds for all three TC cases wherein the changes in intensity are reduced by as much as 35 % and 8 %, respectively. The change in size is also much less in the SST+ATM experiments with changes in TFW ranging from 33 – 60 % in the CESM2_SST experiments while only 1 % - 9 % in the CESM2_SST+ATM experiments. While the changes in rainfall rate reach up to 17 % in the CESM2_SST experiment and only up to 7 % in the CESM2_SST+ATM experiments. Compared with the idealized SST+ experiments, the pattern of SST increases in the CESM2_SST simulations induces a larger intensity change since the TCs

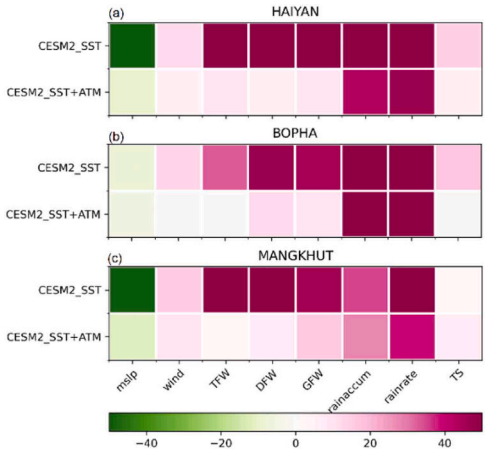

Fig. 10. Percent change relative to the control in TC characteristics in terms of intensity - minimum sea level pressure (mslp); maximum winds (wind); size - typhoon force winds (TFW), damaging force winds (DFW), and gale force winds (GFW); rainfall – total accumulated rainfall (rainaccum) and hourly rainfall rate (rainrate); and translation speed (TS) for the SST and SST+ATM experiments for Typhoons (a) Haiyan, (b) Bopha, and (c) Mangkhut.

track along a more conducive environment as well as the temperature difference between the sea surface and atmosphere.

The substantial increase in TC intensity in the CESM2_SST experiments are largely driven by more heat flux due to warmer SSTs (Fig. 11). The increase in mid-tropospheric relative humidity is also reduced from up to 30 % in the CESM2_SST experiments to only up to 4 % in the CESM2_SST+ATM experiments.

3.3. Radiative-convective equilibrium (RCE) experiments

To further account for the imbalances that might result from imposing SST and ATM deltas, we used another approach wherein we started the simulations in the RCE state (Wang and Toumi, 2018) where storms are simulated under sea surface warming with pre-storm atmospheric adjustments under RCE conditions.

Table 3 shows the changes in intensity and size of the TCs with the

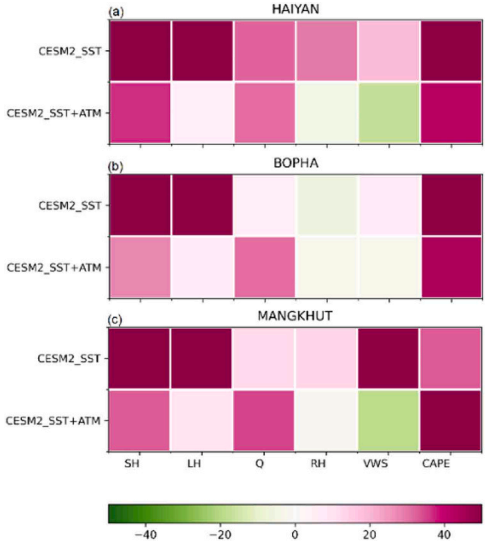

Fig. 11. Percent change relative to the current climate in sensible (SH) and latent heat flux (LH), water vapor mixing ratio (Q), relative humidity (RH), vertical wind shear (VWS) and convective available potential energy (CAPE) for the SST and SST+ATM experiments for Typhoons (a) Haiyan, (b) Bopha, and (c) Mangkhut.

Experiments with SST warming of 2℃ with an additional spin-up time of 15 days (for Haiyan only, SST+2_-15days), 10 days (SST+2_-10days) and experiments under stable relative humidity (SST+2_rh) for the three TC cases. The changes in intensity and size are smaller in the experiments with stable relative humidity, in particular, the percent changes in the maximum winds for Haiyan are 4.0 (2.0), Bopha is 4.0 (2.3), and Mangkhut 9.7 (7.4) for the SST+2 (SST+2_rh) experiments; and the size (GFW) is 13 (1.2) for Haiyan, 0 (-0.4) for Bopha, and 25 (4.3) for Mangkhut.

In the time series of the latent heat flux (Fig. 12), one can see that the LHF increases dramatically in the first two days of all the simulations. From simulation hour 48, the fluxes fluctuate around some mean value. The LHF increased dramatically regardless of the lead times (-15 days and −10 days) in the SST+2 experiments. Modest increases in LHF can be seen in the SST+2_rh experiments, which may be due to the modest changes in intensity in these experiments.

Based on these results, TCs are generally less sensitive to changes in SST when simulated under near - RCE conditions with smaller changes in intensity and size, as highlighted by Wang and Toumi (2018). Additionally, several numerical experiments conducted by Sun et al. (2014) and Sun et al. (2013) looked into the dynamic and thermodynamic effects of SST on TC intensity. Sun et al. (2014) found that variations in inner and outer SST exert opposing effects on TC intensity, with inner SST increases enhancing TC intensity and reducing inner-core size, while outer SST increases have the opposite effect. This underscores the importance of understanding the mechanisms governing TC intensity response to SST changes. Sun et al. (2013) further investigated the effects of relative and absolute SST on TC intensity, highlighting the significance of relative SST within a specific radius of the TC center in influencing TC intensity. Their findings suggest that TC intensity is more sensitive to relative SST rather than absolute SST due to changes in air-sea temperature and moisture differences.

The results from the last experimental design provide additional insights into the response of damaging TCs to SST warming in the region surrounding the Philippines. In the simulations that used pre-storm atmospheric adjustments, the TCs showed less sensitivity to the changes in SST, as compared to those without pre-storm adjustments, that is, a dampened response of TCs to SST changes. More specifically, the last set of simulations demonstrated smaller changes in peak intensity, with an average reduction of 7.33 % change per ℃ and in size (GFW), with an average reduction of 11 % change per ℃ for all TC cases. These findings suggest that atmospheric conditions prior to TC formation play a critical role in modulating the response of TCs to SST warming. From the point of view of building simulation and prediction capacity for the Philippines, this highlights the importance of considering atmospheric stability in understanding and predicting the impacts of SST warming on TC behavior, a finding not yet found in studies that aim to predict the changing nature of TCs impacting the Philippines.

Table 3
Percent change per ℃ change in intensity and size based on the experiments with SST warming of 2℃(SST+2), experiments with an additional spin-up time of 15 days (for Haiyan only, SST+2_-15days), 10 days (SST+2_-10days) and experiments under stable relative humidity (SST+2_rh) for the three TC cases.

Experiments	Intensity (Wind)	Size (GFW)
HAIYAN		
SST+2	4.0	13
SST+2_-15days	4.8	11
SST+2_-10days	3.8	10
SST+2_rh	2.0	1.2
BOPHA		
SST+2	4.0	0
SST+2_-10days	2.0	
SST+2_rh	2.3	-0.4
MANGKHUT		
SST+2	9.7	25
SST+2_-10days	9.7	24
SST+2_rh	7.4	4.3

4. Summary and conclusion

This study uses sensitivity analysis to investigate the influence of imposed SST anomalies on three of the most damaging TCs in the Philippines – Typhoon Haiyan (2013), Typhoon Bopha (2012) and Typhoon Mangkhut (2018), recognizing how SST changes are an important future uncertainty affecting TC risk. The added value of this study is that it complements the imposition of a full future scenario, by using three different, and independent, approaches in order to understand the response of TCs to imposed climate change. A set of simulations with uniform SST anomalies applied (+4, +2, +1, 0, −1, −2, −4°C) to show the influence of SST on TC characteristics (track, size, intensity, rainfall). Additional experiments using delta from CESM2 for SST and ATM in the far future, and, finally, with the three TC cases under RCE were also conducted. Unlike previous studies that often focus on a single approach, this study utilizes three different and independent methodologies to understand TC response to imposed climate change.

The results of the sensitivity experiments are presented, including changes in TC track, size, intensity, rainfall, translation speed, and environmental variables such as relative humidity, surface latent heat flux, water vapor mixing ratio, and vertical wind shear. The study finds that increasing SSTs lead to northward shifts in TC tracks, intensification of TCs, and increases in TC-associated rainfall. Additionally, the study examines the influence of atmospheric temperature changes on TC characteristics, showing that pronounced changes occur in TC properties when only SST anomalies are considered, while smaller changes are observed when changes in atmospheric temperature profiles are also imposed. TCs that intensify as a result of an increased SSTs tend to track northward as a result of the enhanced steering flow (Katsube and Inatsu, 2016) and weakening of the Western North Pacific Subtropical High (Ren et al., 2014). The TCs in the warmer SST experiments also became larger (in terms of the different wind thresholds) relative to the CTRL experiment, which results in a stronger beta drift effect so that the TCs have a greater tendency to drift poleward (Emanuel, 2015; Parker et al.2018).

The increase in SSTs results in an increase in intensity and TC-associated precipitation. The difference in the SST+4 experiment relative to the CTRL for maximum wind speeds reached 47, 46, and 39 m/s for Haiyan, Bopha, and Mangkhut, respectively. The minimum central pressure dropped to as low as 846 hPa for Haiyan, 903 hPa for Bopha, and 830hPa for Mangkhut in the SST+4 runs. Analysis of the accumulated rainfall and rainfall rates also showed that, as SST increases (decreases), the amount of rainfall also increases (decreases).

The pronounced changes observed in TC characteristics in the CESM2_SST experiments, particularly in terms of intensity, size, and rainfall, underscore the significant influence of SST on TC characteristics. The substantial increase in TC intensity in the CESM2_SST experiments is primarily attributed to the enhanced heat flux resulting from warmer SSTs. This increased heat flux provides additional energy for TC intensification, leading to higher wind speeds and lower minimum sea level pressure. However, the CESM2_SST+ATM experiments showed relatively smaller changes in TC characteristics compared to the CESM2_SST experiments. This suggests that the atmospheric adjustments imposed in the SST+ATM experiments mitigate the intensification of TCs driven solely by warmer SSTs. By modifying the atmospheric temperature profile, the SST+ATM experiments maintain a more stable atmospheric environment, which limits the magnitude of TC intensity changes.

In contrast, the RCE experiments-initiated simulations under conditions of radiative-convective equilibrium, where TCs are simulated under sea surface warming with pre-storm atmospheric adjustments. These experiments aimed to account for imbalances resulting from imposing SST and ATM deltas. The results of the RCE experiments indicate that TCs are generally less sensitive to changes in SST when

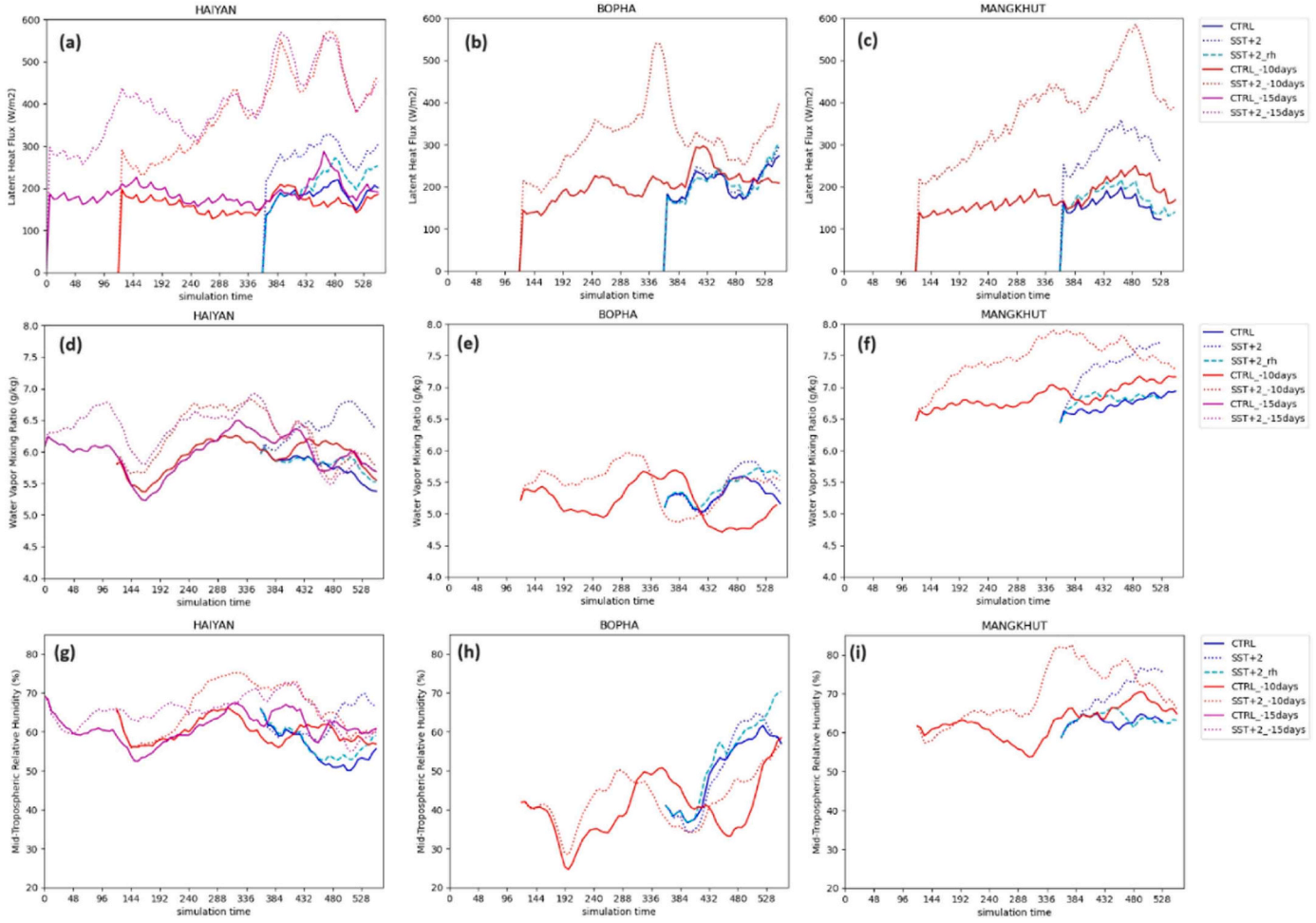

Fig. 12. Time series of the simulated latent heat flux (W m-2), water vapour mixing ratio (g/kg), and mid-tropospheric relative humidity (%) of the experiments with SST warming of 2C with an additional spin-up time of 10 days (SST+2_-10days) and experiments under stable relative humidity (SST+2_rh) for the three TC cases (a) Haiyan, (b) Bopha, and (c) Mangkhut.

simulated under near-RCE conditions. The smaller changes in TC intensity and size observed in these experiments suggest that maintaining atmospheric stability through pre-storm atmospheric adjustments dampens the response of TCs to SST warming.

Since this is a highly idealized SST sensitivity study (as in Lavender et al., 2018; Radu et al., 2014; Kilic and Raible, 2013), there are important caveats, since changing the SST without changing other variables such as atmospheric temperature may result in surface energy imbalances (Emanuel and Sobel, 2013) and the simulated changes may not be realistic (Lavender et al., 2018). In addition, the TCs follow different tracks, as they are experiencing different environments with the imposed changes in SSTs. The use of WRF's one-dimensional ocean-mixed layer model also indicates a TC-induced mixed layer cooling during the passage of the TCs (Supplementary Figure 1); however, investigating the sensitivity of the simulated TC intensity and tracks to ocean-mixed layer is beyond the scope of this study. The results in this study provide insights into the role of uncertainty in projections of SST changes (and atmospheric temperature) on the TC characteristics and corresponding cyclone damage potential. Further work to analyse the potential changes in TC characteristics using data from a set of four CMIP6 models is currently underway.

Author statement

We declare that this manuscript is original, has not been published before and is not currently being considered for publication elsewhere. We confirm that the manuscript has been read and approved by all named authors and that there are no other persons who satisfied the criteria for authorship but are not listed. We further confirm that the order of authors listed in the manuscript has been approved by all of us. We understand that the Corresponding Author is the sole contact for the Editorial process. He/she is responsible for communicating with the other authors about progress, submissions of revisions and final approval of proofs.

CRediT authorship contribution statement

Rafaela Jane Delfino: Writing – review & editing, Writing – original draft, Visualization, Validation, Methodology, Investigation, Formal analysis, Data curation, Conceptualization. **Kevin Hodges:** Writing – review & editing, Writing – original draft, Validation, Supervision, Software, Methodology, Formal analysis, Conceptualization. **Pier Luigi Vidale:** Writing – review & editing, Writing – original draft, Validation, Supervision, Resources, Methodology, Investigation, Formal analysis, Conceptualization. **Gerry Bagtasa:** Writing – review & editing, Writing – original draft, Visualization, Validation, Supervision, Resources, Methodology, Formal analysis, Data curation, Conceptualization.

Declaration of Competing Interest

The authors declare that they have no known competing financial interests or personal relationships that could have appeared to influence

the work reported in this paper.

Data Availability

Simulation data are stored at the JASMIN data storage facility and are available upon request from the corresponding author. Code for the WRF model is available at http://www.www2.mmm.ucar.edu/wrf/users/downloads.html. WPS geographical input data are available from https://www.www2.mmm.ucar.edu/wrf/users/download/get_sources_wps_geog.html#mandatory. TRACK is available from https://www.gitlab.act.reading.ac.uk/track/45track. CF-python and CF-plot were used in the analysis and visualization, and installation packages are available from https://www.ncas-cms.github.io/cf-python/.

Acknowledgements

The authors would like to thank Olivia C. Cabrera for some insights on the importance of considering atmosphere-ocean feedback in the experiments. Rafaela Jane Delfino was supported by a scholarship under the Philippine Commission for Higher Education and British Council under the Joint Development of Niche Programme through Philippines-UK Linkages (JDNP) Dual PhD Program. Kevin Hodges and Pier Luigi Vidale is funded by the RCUK through the Natural Environment Research Council. Gerry Bagtasa and Rafaela Jane Delfino are also supported by the Department of Science and Technology - Philippine Council for Industry, Energy, and Emerging Technology Research and Development (DOST-PCIEERD) under the project entitled "Analysis of tropical cyclone rapid intensification in the Philippines: its characteristics, impacts, and future projections" (1211131). This research used resources of the JASMIN data analysis facility supported by CEDA.

Appendix A. Supporting information

Supplementary data associated with this article can be found in the online version at doi:10.1016/j.rsma.2024.103595.

References

Bagtasa, G., 2017. Contribution of tropical cyclones to rainfall in the Philippines. J. Clim. Vol 30, 3621–3633. https://doi.org/10.1175/JCLI-D-16-0150.1.

Bagtasa, G., 2022. Variability of tropical cyclone rainfall volume in the Philippines. Int. J. Climatol. 1 (11) https://doi.org/10.1002/joc.7573.

Bender, M.A., Knutson, T.,R., Tuleya, R.,E., Sirutis, J.,J., Vecchi, G.A., Garner, S.T., Held, I.M., 2010. Modeled impact of anthropogenic warming on the frequency of intense Atlantic hurricanes, 2010 Jan 22 Science 327 (5964), 454–458. https://doi.org/10.1126/science.1180568.

Bi, M., Li, T., 2023. Sensitivity of the size of a TC to Sea Surface temperatures in its outer region. J. Meteorol. Res. 37 (6), 829–840. https://doi.org/10.1007/s13351-023-2185-8.

Brucal, A., Roezer, V., Dookie, D.S., Byrnes, R., Ravago, M.V., and Cruz, F. (2020). Disaster impacts and financing: local insights from the Philippineshttps://www.lse.ac.uk/granthaminstitute/publication/disaster-impacts-and-financing-local-insights-from-the-philippines/.

Cao, X., Watanabe, M., Wu, R., Chen, W., Sun, Y., Yan, Q., Wu, L., 2024. The projected poleward shift of tropical cyclogenesis at a global scale under climate change in MRI-AGCM3. 2H. Geophys. Res. Lett. 51 (3), e2023GL107189.

Cha, E.J., Knutson, T.R., Lee, T.C., Ying, M., Nakaegawa, T., 2020. Third assessment on impacts of climate change on tropical cyclones in the Typhoon Committee Region–Part II: future projections. Trop. Cyclone Res. Rev. 9 (2), 75–86.

Chavas, D.R., Emanuel, K., 2014. Equilibrium tropical cyclone size in an idealized state of axisymmetric radiative–convective equilibrium. J. Atmos. Sci. 71 (5), 1663–1680.

Chen, F., Dudhia, J., 2001. Coupling an advanced land-surface/ hydrology model with the Penn State/NCAR MM5 modeling system. Part I: model description and implementation. Mon. Weather Rev. 129, 569–585. https://doi.org/10.1175/1520-0493(2001)129<0569:CAALSH>2.0.CO;2.

Christensen et al.. (2013). Climate phenomena and their relevance for future regional climate change. In: Stocker et al.et al., eds. Climate Change 2013: The Physical Science Basis. Contribution of Working Group I to the Fifth Assessment Report of the Intergovernmental Panel on Climate Change (IPCC AR5). Cambridge, UK and New York, NY: Cambridge University Press.

Cinco, T.A., de Guzman, R.G., Ortiz, A.M.D., Delfino, R.J.P., Lasco, R.D., Hilario, F.D., Ares, E.D., 2016. Observed trends and impacts of tropical cyclones in the Philippines. Int. J. Climatol. 36 (14) https://doi.org/10.1002/joc.4659.

Climate Prediction Center (CPC), (2021). Cold and Warm Episodes by Season. https://www.origincpcncepnoaagov/products/analysis_monitoring/ensostuff/ONI_v5php.

Comiso, J.C., Perez, G.P., Stock, L.V., 2015. Enhanced Pacific Ocean Sea surface temperature and its relation to Typhoon Haiyan. J. Environ. Sci. Manag. 18 (1), 1–10. ⟨https://ovcre.uplb.edu.ph/journals-uplb/index.php/JESAM/article/view/175⟩.

Danabasoglu, G., Lamarque, J.-F., Bacmeister, J., Bailey, D.A., DuVivier, A.K., Edwards, J., et al., 2020. The Community Earth System Model Version 2 (CESM2). J. Adv. Model. Earth Syst. 12 https://doi.org/10.1029/2019MS001916.

Delfino, R.J.P., Bagtasa, G., Hodges, K., Vidale, P.L.V., 2022. Sensitivity of simulating Typhoon Haiyan (2013) using WRF: the role of cumulus convection, surface flux parameterizations, spectral nudging and initial and boundary conditions. Nat. Hazards Earth Syst. Sci. J. https://doi.org/10.5194/nhess-22-3285-2022.

Delfino, R.J.P., Vidale, P.L., Bagtasa, G., Hodges, K., 2023. Response of damaging tropical cyclone events in the Philippines to climate forcings from selected CMIP6 models using the pseudo global warming technique. Clim. Dyn. https://doi.org/10.1007/s00382-023-06742-6.

Dudhia, J., 1989. Numerical study of convection observed during the Winter Monsoon Experiment using a mesoscale two–dimensional model. J. Atmos. Sci. 46, 3077–3107. https://doi.org/10.1175/1520-0469(1989)046<3077:NSOCOD>2.0.CO;2.

Gallo, F., Daron, J., Macadam, I., Cinco, T., Villafuerte, M., Jones, R.G., … Tucker, S. (2019). High-resolution regional climate model projections of future tropical cyclone activity in the Philippines.1181–1194. https://doi.org/10.1002/joc.5870.

Goddard, L., DeWitt, D.G., Reynolds, R.W., 2009. Practical implications of uncertainty in observed SSTs. L09710 Geophys. Res. Lett. 36. https://doi.org/10.1029/2009GL037703.

Gong, D., Tang, X., Chan, J.C.L., Wang, Q., 2022. Trends of tropical cyclone translation speed over the Western North Pacific during 1980−2018 (available). Atmosphere 13 (6), 896. https://doi.org/10.3390/atmos13060896.

Hegde, A.K., Kawamura, R., Kawano, T., et al., 2016. Evidence for the significant role of sea surface temperature distributions over remote tropical oceans in tropical cyclone intensity. Clim. Dyn. 47, 623–635. https://doi.org/10.1007/s00382-015-2859-8.

Hersbach, H., Bell, B., Berrisford, P., Hirahara, S., Horányi, A., Nicolas, J., Thépaut, J., 2020. The ERA5 global reanalysis, 2020 Q J. R. Meteor. Soc. 146, 1999–2049. https://doi.org/10.1002/qj.3803.

Hill, K.A., Lackmann, G.M., 2011. The impact of future climate change on TC intensity and structure: A downscaling approach. J. Clim. 24, 4644–4661.

Hodges, K., Cobb, A., Vidale, P.L., 2017. How well are Tropical Cyclones represented in reanalysis data sets? ISSN 1520-0442 J. Clim. 30 (14), 5243–5264. https://doi.org/10.1175/JCLI-D-16-0557.1.

Hodges, K.I., Klingaman, N.P., 2019. Prediction errors of tropical cyclones in the western north Pacific in the Met Office global forecast model. ISSN 0882-8156 Weather Forecast. 34 (5), 1189–1209. https://doi.org/10.1175/WAF-D-19-0005.1.

Hong, S.-Y., Lim, J.-O.J., 2006. The WRF single-moment 6-class microphysics scheme (WSM6). J. Korean Meteor Soc. 42, 129–151.

Isaksen, L., Bonavita, M., Buizza, R., Fisher, M., Haseler, J., Leutbecher, M., Raynaud, L., 2010. Ensemble of Data Assimilations at ECMWF. Technical Memorandum 636. ECMWF, Reading, UK. ⟨https://www.ecmwf.int/en/elibrary/10125-ensemble-data-assimilations-ecmwf⟩.

Ito, R., Takemi, T., Arakawa, O., 2016. A possible reduction in the severity of typhoon wind in the northern part of Japan under global warming: a case study. Sola 12, 100–105.

Japan Meteorological Agency (JMA) (2012). Annual Report on the Activities of the RSMC Tokyo -Typhoon Center 2012. https://www.jma.go.jp/jma/jma-eng/jma-center/rsmc-hp-pubeg/AnnualReport/2012/Text/Text2012.pdf.

Japan Meteorological Agency (JMA) (2013). Annual Report on the Activities of the RSMC Tokyo -Typhoon Center 2013. https://www.jma.go.jp/jma/jma-eng/jma-center/rsmc-hp-pub-eg/AnnualReport/2013/Text/Text2013.pdf.

Japan Meteorological Agency (JMA) (2018). Annual Report on the Activities of the RSMC Tokyo -Typhoon Center 2018 https://www.jma.go.jp/jma/jma-eng/jma-center/rsmc-hp-pub-eg/AnnualReport/2018/Text/Text2018.pdf.

Kanada, S., Aiki, H., Tsuboki, K., Takayabu, I., 2021. Future changes of a slow-moving intense typhoon with global warming: a case study using a regional 1-km-mesh atmosphere–ocean coupled model. SOLA 17A, 14–20. https://doi.org/10.2151/sola.17A-003.

Katsube, K., Inatsu, M., 2016. Response of Tropical Cyclone Tracks to Sea Surface Temperature in the Western North Pacific. J. Clim. 29 (5), 1955–1975. ⟨https://journals.ametsoc.org/view/journals/clim/29/5/jcli-d-15-0198.1.xml⟩.

Kilic, C., Raible, C., 2013. Investigating the sensitivity of hurricane intensity and trajectory to sea surface temperatures using the regional model WRF. Meteorol. Z. 22, 685–698.

Knutson, T., Camargo, S.J., Chan, J.C.L., Emanuel, K., Ho, C., Kossin, J., Mohapatra, M., Satoh, M., Sugi, M., Walsh, K., Wu, L., 2019. Tropical Cyclones and Climate Change Assessment: Part I: detection and attribution. Bull. Am. Meteorol. Soc. 100 (10), 1987–2007. ⟨https://journals.ametsoc.org/view/journals/bams/100/10/bams-d-18-0189.1.xml⟩.

Knutson, T., Camargo, S.J., Chan, J.C., Emanuel, K., Ho, C.H., Kossin, J., Wu, L., 2020. Tropical cyclones and climate change assessment: Part II: projected response to anthropogenic warming. BAMS 101 (3), E303–E322.

Knutson, T.R., Tuleya, R.E., 2004. Impact of CO2-induced warming on simulated hurricane intensity and precipitation: sensitivity to the choice of climate model and convective parameterization. J. Clim. 17 (18), 3477–3495. https://doi.org/10.1175/2011JCLI3761.1.

Knutson, T.R., Tuleya, R.E., Kurihara, Y., 1998. Simulated increase of hurricane intensities in a CO2-warmed climate. Science 279 (5353), 1018–1021.

Kossin, J.P., 2018. A global slowdown of tropical-cyclone translation speed. Nature 558, 104–107.
Lackmann, G.M., 2015. Hurricane Sandy before 1900 and after 2100. BAMS 96 (4), 547–560.
Lara, T. (2020). The most destructive typhoons in the Philippines ⟨https://philstarlife.com/news-and-views/755589-most-destructive-typhoons-ph-typhoon-rolly?page=4⟩.
Lai, Y., Li, J., Gu, X., Chen, Y.D., Kong, D., Gan, T.Y., Wu, G., 2020. Greater flood risks in response to slowdown of tropical cyclones over the coast of China. Proc. Natl. Acad. Sci. 117 (26), 14751–14755.
Lavender, S.L., Hoeke, R.K., Abbs, D.J., 2018. The influence of sea surface temperature on the intensity and associated storm surge of tropical cyclone Yasi: a sensitivity study. Nat. Hazards Earth Syst. Sci. 18, 795–805. https://doi.org/10.5194/nhess-18-795-2018.
Lenderink, G., Belušić, D., Fowler, H.J., Kjellström, E., Lind, P., van Meijgaard, E., van Ulft, B., de Vries, H., 2019. Systematic increases in the thermodynamic response of hourly precipitation extremes in an idealized warming experiment with a convection-permitting climate model. Environ. Res Lett. 2019 14 (7), 074012.
Li, F., Song, J., Li, X., 2018. preliminary evaluation of the necessity of using a cumulus parameterization scheme in high-resolution simulations of Typhoon Haiyan (2013). Nat. Hazards 92, 647–667. https://doi.org/10.1007/s11069-018-3218-y.
Liu, M., Vecchi, G.A., Smith, J.A., et al., 2019. Causes of large projected increases in hurricane precipitation rates with global warming. npj Clim. Atmos. Sci. 2 (1), 1–5.
Lyon, B., Camargo, S.J., 2009. The seasonally-varying influence of ENSO on rainfall and tropical cyclone activity in the Philippines. Clim. Dyn. 32, 125–141. https://doi.org/10.1007/s00382-008-0380-z.
Mejia, J.F., Koračin, D., Wilcox, E.M., 2018. Effect of coupled global climate models sea surface temperature biases on simulated climate of the western United States. Int J. Clim. 38, 5386–5404. https://doi.org/10.1002/joc.5817.
Mlawer, Eli J., Steven. J.Taubman, Patrick. D.Brown, M.J. Iacono, and S.A. Clough (1997). Radiative transfer for inhomogeneous atmospheres: RRTM, a validated correlated–k model for the longwave. J. Geophys. Res., 102, 16663–16682. doi: 10.1029/97JD00237.
Monin, A.S., Obukhov, A.M., 1954. Basic laws of turbulent mixing in the surface layer of the atmosphere. Contrib. Geophys Inst. Acad. Sci. USSR 151, 163–187 https://gibbs.science/efd/handouts/monin_obukhov_1954.pdf.
Nakamura, J., Camargo, S.J., Sobel, A.H., Henderson, N., Emanuel, K.A., Kumar, A., LaRow, T.E., Murakami, H., Roberts, M.J., Scoccimarro, E., Vidale, P.L., Wang, H., Wehner, M.F., Zhao, M., 2017. Western North Pacific tropical cyclone model tracks in present and future climates. J. Geophys. Res. Atmos. 122 (18) https://doi.org/10.1002/2017jd027007.
Nakamura, R., Shibayama, T., Esteban, M., Iwamoto, T., 2016. Future typhoon and storm surges under different global warming scenarios: case study of typhoon Haiyan (2013). Nat. Hazards 82, 1645–1681.
National Disaster Risk Reduction and Managament Council (NDRRMC) (2012). NDRRMC Update: SitRep No.38 re Effects of Typhoon Pablo (Bopha). 25 December 2012, 6: 00AM. https://reliefweb.int/sites/reliefweb.int/files/resources/NDRRMC%20Updat%20Sitrep%20No%2038%20re%20Effects%20of%20Typhoon%20Pablo%20Bopha.pdf.
National Oceanic and Atmospheric Administration (NOAA) (2018). National Centers for Environmental Information Global Climate Report – September 2018. ⟨https://www.ncdc.noaa.gov/sotc/global/201809⟩.
NDRRMC (2014). Final Report re: Effects of Typhoon Yolanda (Haiyan). https://ndrrmc.gov.ph/attachments/article/1329/FINAL_REPORT_re_Effects_of_Typhoon_YOLANDA_(HAIYAN)_06-09NOV2013.pdf.
NDRRMC (2018). NDRRMC Update: SitRep No.57 re Preparedness Measures: Effects for TY OMPONG as of 0600H 06OCT2018.pdf ⟨https://ndrrmc.gov.ph/attachments/article/3437/SitRep_No_57_re_Preparedness_Measures_Effects_for_TY_OMPONG_as_of_0600H_06OCT2018.pdf⟩.
NOAA (2021). National Weather Service Climate Prediction Center's Cold & Warm Episodes by Season ⟨https://www.ncdc.noaa.gov/sotc/global/201809⟩.
National Oceanic, Atmospheric Administration (NOAA). https://www.ncdc.noaa.gov/sotc/global/201809. (Accessed September 2018).
Nolan, D.S., Rappin, E.D., Emanuel, K.A., 2007. Tropical cyclogenesis sensitivity to environmental parameters in radiative–convective equilibrium. Q. J. R. Meteorol. Soc.: A J. Atmos. Sci., Appl. Meteorol. Phys. Oceanogr. 133 (629), 2085–2107.
Parker, C.L., Bruyère, C.L., Mooney, P.A., Lynch, A.H., 2018. The response of land-falling tropical cyclone characteristics to projected climate change in northeast Australia, 0 (0), 0 Clim. Dyn.. https://doi.org/10.1007/s00382-018-4091-9.
Patricola, C.M., Wehner, M.F., 2018. Anthropogenic influences on major tropical cyclone events. Nature. https://doi.org/10.1038/s41586-018-0673-2.
Philippine Atmospheric, Geosicences, Astronomical Services Adminsitration (PAGASA). (2018) Typhoon Ompong (Mangkhut/1822) Summary Report ⟨https://pubfiles.pagasa.dost.gov.ph/pagasaweb/files/tamss/weather/tcsummary/TY_Ompong_Mangkhut.pdf⟩.
Powers, J.G., Klemp, J.B., Skamarock, W.C., Davis, C.A., Dudhia, J., Gill, D.O., Coen, J.L., Gochis, D.J., Ahmadov, R., Peckham, S.E., Grell, G.A., Michalakes, J., Trahan, S., Benjamin, S.G., Alexander, C.R., Dimego, G.J., Wang, W., Schwartz, C.S., Romine, G. S., Liu, Z., Snyder, C., Chen, F., Barlage, M.J., Yu, W., Duda, M.G., 2017. The weather research and forecasting model: overview, system efforts, and future directions. Bull. Am. Meteor. Soc. 98, 1717–1737. https://doi.org/10.1175/BAMS-D-15-00308.1.
Radu, R., Toumi, R., Phau, J., 2014. Influence of atmospheric and sea surface temperature on the size of hurricane Catarina. Q. J. R. Meteorol. Soc. 140, 1778–1784. https://doi.org/10.1002/qj.2232.
Ren, D., Lynch, M., Leslie, L.M., Lemarshall, J., 2014. Sensitivity of tropical cyclone tracks and intensity to ocean surface temperature: Four cases in four different basins. Tellus A: Dyn. Meteorol. 66 (1), 24212.
Schär, C., Frei, C., Lüthi, D., Davies, H.C., 1996. Surrogate climate-change scenarios for regional climate models. Geophys. Res. Lett. 23 (6), 669–672, 10.1029/96GL00265.
Scoccimarro, E., 2016. Modeling tropical cyclones in a changing climate. Oxf. Res. Encycl.: Nat. Hazard Sci. https://doi.org/10.1093/acrefore/9780199389407.013.2.
Roberts, M.J., Camp, J., Seddon, J., Vidale, P.L., Hodges, K., Vannière, B., Mecking, J., Haarsma, R., Bellucci, A., Scoccimarro, E., Caron, L.-P., Chauvin, F., Terray, L., Valcke, S., Moine, M.-P., Putrasahan, D., Roberts, C.D., Senan, R., Zarzycki, C., Ullrich, P., Yamada, Y., Mizuta, R., Kodama, C., Fu, D., Zhang, Q., Danabasoglu, G., Rosenbloom, N., Wang, H. and Wu, L. (2020) Projected future changes in tropical cyclones using the CMIP6 HighResMIP multimodel ensemble. Geophysical Research Letters, 47 (14). e2020GL088662. ISSN 0094-8276 doi: https://doi.org/10.1029/2020gl088662.
Skamarock W.C., Klemp J.B., Dudhia J., Gill D.O., Barker D.M., Duda M., Huang X.-Y., Wang W., Powers J.G. (2008) A description of the advanced research WRF version 3. NCAR Technical Note, NCAR/TN-475STR, National Center for Atmospheric Research, Boulder, Colorado.
Sun, Y., Zhong, Z., Ha, Y., Wang, Y., Wang, X., 2013. The dynamic and thermodynamic effects of relative and absolute sea surface temperature on tropical cyclone intensity. Acta Meteorol. Sin. 27 (1), 40–49.
Sun, Y., Zhong, Z., Li, T., Yi, L., Camargo, S.J., Hu, Y., Shi, J., 2017a. Impact of ocean warming on tropical cyclone track over the western north pacific: a numerical investigation based on two case studies. J. Geophys. Res. Atmos. 122 (16), 8617–8630.
Sun, Y., Zhong, Z., Li, T., Yi, L., Hu, Y., Wan, H., Li, Q., 2017b. Impact of ocean warming on tropical cyclone size and its destructiveness. Sci. Rep. 7 (1), 8154.
Sun, Y., Zhong, Z., Yi, L., Ha, Y., Sun, Y., 2014. The opposite effects of inner and outer sea surface temperature on tropical cyclone intensity. J. Geophys. Res. Atmos. 119 (5), 2193–2208.
Takayabu, I., Hibino, K., Sasaki, H., Shiogama, H., Mori, N., Shibutani, Y., Takemi, T., 2015. Climate change effects on the worst-case storm surge: a case study of Typhoon Haiyan. Environ. Res. Lett. 10 (6), 064011.
Tewari, M., Chen, F., Wang, W., Dudhia, J., LeMone, M.A., Mitchell, K., Ek, M., Gayno, G., Wegiel, J., Cuenca, R.H., 2004. Implementation and verification of the unified NOAH land surface model in the WRF model. 20th Conf. Weather Anal. Forecast. /16th Conf. Numer. Weather Predict. 11–15. ⟨https://ams.confex.com/ams/84Annual/techprogram/paper_69061.htm⟩.
Tompkins, A.M., Craig, G.C., 1998. Radiative–convective equilibrium in a three-dimensional cloud-ensemble model. Q. J. R. Meteorol. Soc. 124 (550), 2073–2097.
Trenberth, K.E., Cheng, L., Jacobs, P., Zhang, Y., Fasullo, J., 2018. Hurricane Harvey links to ocean heat content and climate change adaptation. Earth'S. Future 6 (5), 730–744.
Villafuerte, I.I., Lambrento, M.Q., Hodges, J.C.R., Cruz, K.I., Cinco, F.T., T. A, Narisma, G.T., 2021. Sensitivity of tropical cyclones to convective parameterization schemes in RegCM4. Clim. Dyn. https://doi.org/10.1007/s00382-020-05553-3.
Walsh, K.J.E., Camargo, S.J., Knutson, T.R., et al., 2019. Tropical cyclones and climate change. Trop. Cyclone Res. Rev. 8 (4), 240–250. https://doi.org/10.1016/j.tcrr.2020.01.004.
Walsh, K.J.E., McBride, J.L., Klotzbach, P.J., Balachandran, S., Camargo, S.J., Holland, G., Knutson, T.R., Kossin, J.P., Lee, T., Sobel, A., Sugi, M., 2015. Tropical cyclones and climate change, 2015 WIREs Clim. Change. https://doi.org/10.1002/wcc.371.
Wang, S., Toumi, R., 2018. Reduced sensitivity of tropical cyclone intensity and size to sea surface temperature in a radiative-convective equilibrium environment. Adv. Atmos. Sci. 35 (8), 981–993. https://doi.org/10.1007/s00376-018-7277-5.
Xu, J., Wang, Y., Tan, Z., 2016. The Relationship between Sea Surface Temperature and Maximum Intensification Rate of Tropical Cyclones in the North Atlantic. J. Atmos. Sci. 73 (12), 4979–4988. ⟨https://journals.ametsoc.org/view/journals/atsc/73/12/jas-d-16-0165.1.xml⟩.
Yablonsky, R.M., Ginis, I., 2009. Limitation of one-dimensional ocean models for coupled hurricane-ocean model forecasts. Mon. Wea. Rev. 137, 4410–4419. https://doi.org/10.1175/2009MWR2863.1.
Ying, M., Knutson, T.R., Kamahori, H., & Lee, T. (2012). Impacts of Climate Change on Tropical Cyclones in the Western North Pacific Basin. Part II: Late twenty-first Century Projections, 231–241. https://doi.org/10.6057/2012TCRR02.09.
Yonson, R., Gaillard, J.C., Noy, I., 2016. School of Economics and Finance, Victoria Business School. Available from. Meas. Disaster risk: Ex. Trop. Cyclones Philipp. ⟨www.victoria.ac.nz/sef⟩.
Zhang, G., Murakami, H., Knutson, T.R., Mizuta, R., Yoshida, K., 2020. Tropical cyclone motion in a changing climate. Sci., Adv. 6, 7610. https://doi.org/10.1126/sciadv.aaz7610.